

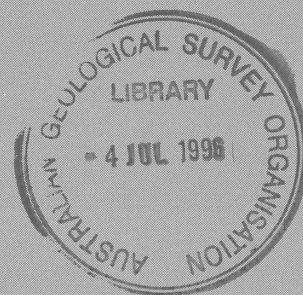
1996/21
C2

METHODS AND CODES USED IN SEISMIC TOMOGRAPHY

BMR PUBLICATIONS COMPACTUS
(LENDING SECTION)

by

Nicholas Rawlinson



RECORD 1996/21

AGSO



AUSTRALIAN
GEOLOGICAL SURVEY
ORGANISATION

BMR COMP
1996/21
C2



AGSO RECORD 1996/21

**METHODS AND CODES USED IN
SEISMIC TOMOGRAPHY**

by

Nicholas Rawlinson



DEPARTMENT OF PRIMARY INDUSTRIES AND ENERGY

Minister for Primary Industries and Energy: Hon. J. Anderson, M.P.

Minister for Resources and Energy: Senator the Hon. W.R. Parer

Secretary: Paul Barratt

AUSTRALIAN GEOLOGICAL SURVEY ORGANISATION

Executive Director: Neil Williams

© Commonwealth of Australia 1996

ISSN: 1039-0073

ISBN: 0 642 24960 1

This work is copyright. Apart from any fair dealings for the purposes of study, research, criticism or review, as permitted under the *Copyright Act 1968*, no part may be reproduced by any process without written permission. Copyright is the responsibility of the Executive Director, Australian Geological Survey Organisation. Requests and inquiries concerning reproduction and rights should be directed to the **Principal Information Officer, Australian Geological Survey Organisation, GPO Box 378, Canberra City, ACT, 2601.**

It is recommended that this publication is referred to as:

RAWLINSON, N., 1996. Methods and Codes used in Seismic Tomography. Australian Geological Survey Organisation, Record 1996/21.

CONTENTS

SUMMARY	1
INTRODUCTION	2
1 THE SEISMIC TOMOGRAPHY METHOD	3
1.1 Model Parameterization	4
1.2 Solving the Forward Problem	6
1.2.1 Shooting Method	7
1.2.2 Bending Method	7
1.2.3 Finite-Difference Method	8
1.2.4 Network Method	12
1.3 Solving the Inverse Problem	14
1.3.1 Algebraic Reconstruction Technique (ART)	17
1.3.2 Simultaneous Iterative Reconstruction Technique (SIRT)	17
1.3.3 Least Squares QR (LSQR) and Conjugate Gradients	18
1.3.4 Global Optimization Techniques	19
2 SEISMIC TOMOGRAPHY SOFTWARE	22
2.1 “Dogstomo” Software Package	22
2.1.1 Solving the Tomographic Problem with “Dogstomo”	23
2.1.2 Methods used to Solve the Forward and Inverse Problem	25
2.2 3-D Tomographic Inversion Code by John Hole	28
2.2.1 Solving the Forward Problem	29
2.2.2 Solving the Inverse Problem	30

2.2.3 Examples of Code Applications	30
2.3 Other Related Software	31
ACKNOWLEDGEMENTS	33
REFERENCES	33
APPENDIX 1: Bibliography	36
3-D Tomography	37
2-D Tomography	39
Teleseismic Tomography	41
Miscellaneous	42
APPENDIX 2: Contacts	44

SUMMARY

AGSO has recently completed several seismic refraction and wide-angle reflection surveys that have also collected data suitable for interpretation by three-dimensional tomographic inversion methods. The survey areas include Tasmania and Mount Isa. This report is designed to act as a guide when the tomographic problem needs to be solved. Methods that are commonly used in each step of the solution process are briefly outlined and several codes designed specifically for three-dimensional tomography are described. In addition, a bibliography of 97 references and many contact addresses are provided for further investigation. The focus of this report is on controlled source travel time tomography.

INTRODUCTION

Seismic tomography presently exists as a popular tool for modelling the Earth's interior. Its origin as a useful method was in the mid 1970's when Aki and others used seismic data from local earthquakes (Aki and Lee, 1976) and teleseismic events (Aki *et al.*, 1977) to determine the velocity structure of portions of the crust using three dimensional inversion techniques. Since then, the evolution of seismic tomography has been rapid, with the development of many new inversion methods including ART (Algebraic Reconstruction Technique), SIRT (Simultaneous Iterative Reconstruction Technique) and Least Squares QR (LSQR), a conjugate gradient technique. More recently, stochastic methods such as the Monte Carlo method, genetic algorithms and Simulated Annealing have been successfully applied to the tomographic problem.

The aim of this report is to provide an overview of tomographic methods for seismic data, with an emphasis on three-dimensional controlled source (eg: airguns, explosions) travel time tomography. To help facilitate this aim, the report has been divided into three sections.

The first section consists of a summary of the steps that are normally necessary in order to obtain a tomographic image, as well as a brief description of some of the methods commonly used for each step. The second section gives a description of some of the software that can be used to help solve the tomographic problem. Two appendices are provided at the end of the report; this constitutes the third section. The first appendix gives a list of 97 references on seismic tomography. These references are mainly journal articles from 1990 onwards and represent some of the latest developments in the field. The second appendix provides a list of some of the leading proponents in seismic tomography. Included are descriptions of research interests and addresses (email and/or internet).

These appendices act as a further source of information if the material contained in the first two sections is insufficiently detailed for the reader. Hopefully, this report will be useful to most people interested in seismic tomography.

1 THE SEISMIC TOMOGRAPHY METHOD

The word “tomo” is from the Greek word which means “slice”. Thus, “tomography” literally means “slice picture”. In its geophysical context, the term “tomography” has been appropriated from the medical technology which images the internal density distribution of the human body using X-rays. While seismic tomography shares some similarities with its medical counterpart, namely the reconstruction of an internal property from line integrals, there are several inherent differences. Principle among these differences is that the ray path of an X-ray through the human body is a straight line. This means that the two-dimensional (2-D) image constructed will always be a true representation of the internal property and that the central slice theorem can justifiably be used to construct a three-dimensional (3-D) image (Lee and Pereyra, 1993). In seismic tomography, the raypath between two points is generally not a straight line. This means that the velocity structure of the subsurface determines whether or not the ray path(s) between a source and receiver lies in the plane of interest. If they do, then a 2-D image reconstruction from line integrals is legitimate. If not, then while it often may be acceptable to reconstruct a 2-D image, it is usually better to reconstruct a 3-D image from the line integrals; this often occurs in the case of strong lateral heterogeneities. Consequently, geophysicists use “seismic tomography” to describe 2-D and 3-D imaging (Hole, 1992).

Tomography may be viewed as a subset of inverse theory (Stewart, 1991) and for this reason, when we speak of seismic tomography it is implicit that inversion is involved. The methodology used to solve a seismic tomography problem normally involves the following steps:

- 1) Model parameterization : Specification of a minimal set of model parameters whose values characterise the system.
- 2) Forward Modelling: Calculating the results of some observable quantity when the values of the model parameters are given.
- 3) Inverse Modelling: Use of the actual measurements of the observable quantity to infer more accurate values of the model parameters.

Some assessment of solution quality is usually made once step 3 is completed. In the case of travel time tomography, the model is parameterized in terms of velocity. The forward modelling involves determining ray paths and travel times between sources and receivers given a velocity model. The inverse problem minimises the difference between predicted and observed travel times by perturbing the velocity model. What follows are brief descriptions of some of the methods used in each of the three steps.

1.1 Model Parameterization

The parameterization employed in a tomographic problem is connected to the forward and inverse modelling technique used. Consequently, it should be chosen with regard to these later procedures as well as the nature of the subsurface determined by any *a priori* information. In travel time tomography, a wide variety of approaches have been used to represent the Earth's velocity structure. Aki and Lee (1976) used a constant velocity block approach in which the subsurface is treated as an array of cells (Figure 1), each with a uniform velocity. This simple approach has the disadvantage of not being able to faithfully represent lateral velocity discontinuities, as well as, from an inverse theory point of view, being both over-determined and under-parameterized (Thurber, 1993). If many thousands of blocks are used, then these problems may be abridged, although computational difficulties may arise.

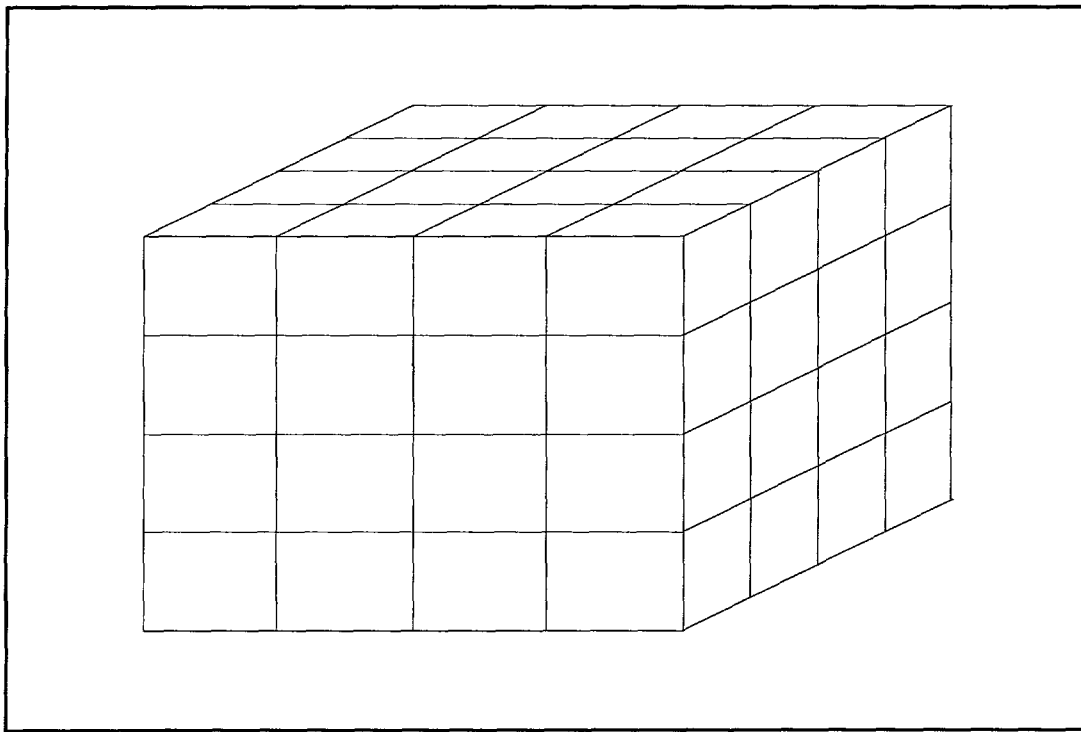


Figure 1: Constant velocity block parameterization. Each block has a constant velocity v_i assigned to it. In this case, $i = 1, 2, 3, \dots, 64$.

Hawley *et al.* (1981) modelled the velocity structure of the crust using flat-lying constant thickness layers subdivided into rectangular blocks, with the velocity being constant in the vertical direction in each layer but varying according to an interpolation function in the horizontal. This interpolation of velocities smoothly varies the velocity between each block within the layer. The interpolation is performed between velocity nodes that are defined along lines that pass vertically through the center of each block (figure 2). The elimination of these horizontal discontinuities is necessary because they introduce unrealistic ray path shadow zones at the surface. Vertical velocity discontinuities

between layers are retained to allow for the existence of head waves. Thus, a set of n two-dimensional velocity functions defines the three-dimensional velocity structure of an n -layered model.

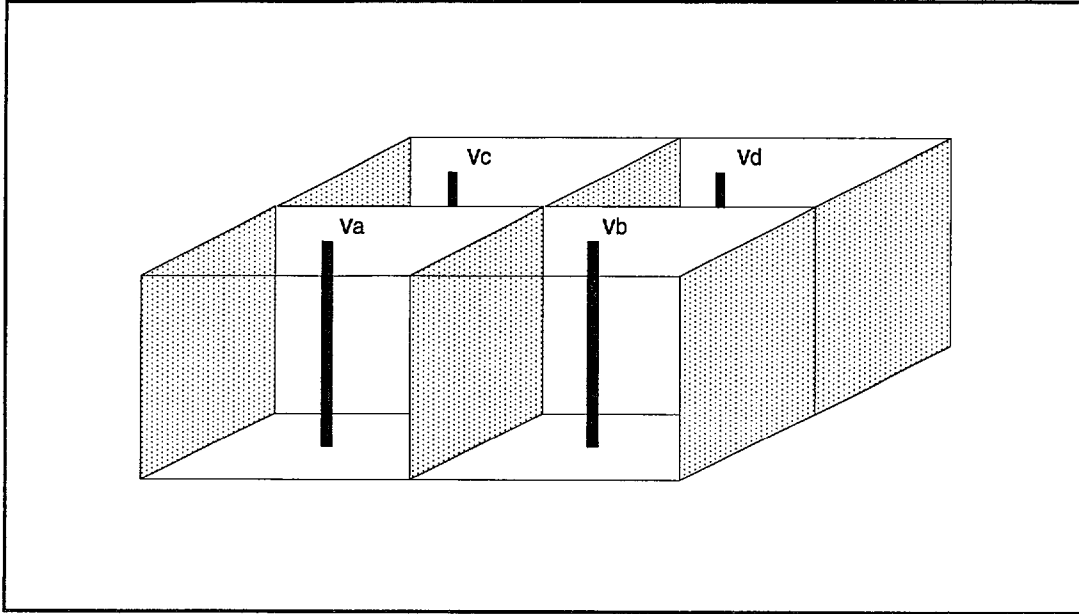


Figure 2: Interpolation is performed between vertical velocity lines v_j .

An alternative to block parameterization is the grid approach used by Thurber (1983). The velocity is defined at each node point of the grid (figure 3) and linear B-spline interpolation is used between the nodes so that the velocity can vary continuously in all directions. The B-spline interpolation function used to find the velocity at a point (x,y,z) is

$$V(x,y,z) = \sum_{i=1}^2 \sum_{j=1}^2 \sum_{k=1}^2 V(x_i, y_j, z_k) \left[\left(1 - \left| \frac{x-x_i}{x_2-x_1} \right| \right) \left(1 - \left| \frac{y-y_j}{y_2-y_1} \right| \right) \left(1 - \left| \frac{z-z_k}{z_2-z_1} \right| \right) \right] \quad (1)$$

where (x_i, y_j, z_k) represent the coordinates for the eight grid points surrounding the point (x,y,z) . Cubic B-spline interpolation may also be used and is especially useful to describe a smooth model when only a small number of nodes exist. However, to avoid undesirable side effects, care must be taken in choosing a starting cubic B-spline model for tomographic inversion. Forcing the model to pass through nodes can induce fluctuation and, sometimes, gradient reversal. These can be transferred to the final results of a tomographic inversion and introduce an undesirable bias. Hence, any starting structure should be inspected for such fluctuations. Shalev (1993) outlines some of the problems associated with the translation to cubic B-spline parameterization and suggests some possible solutions.

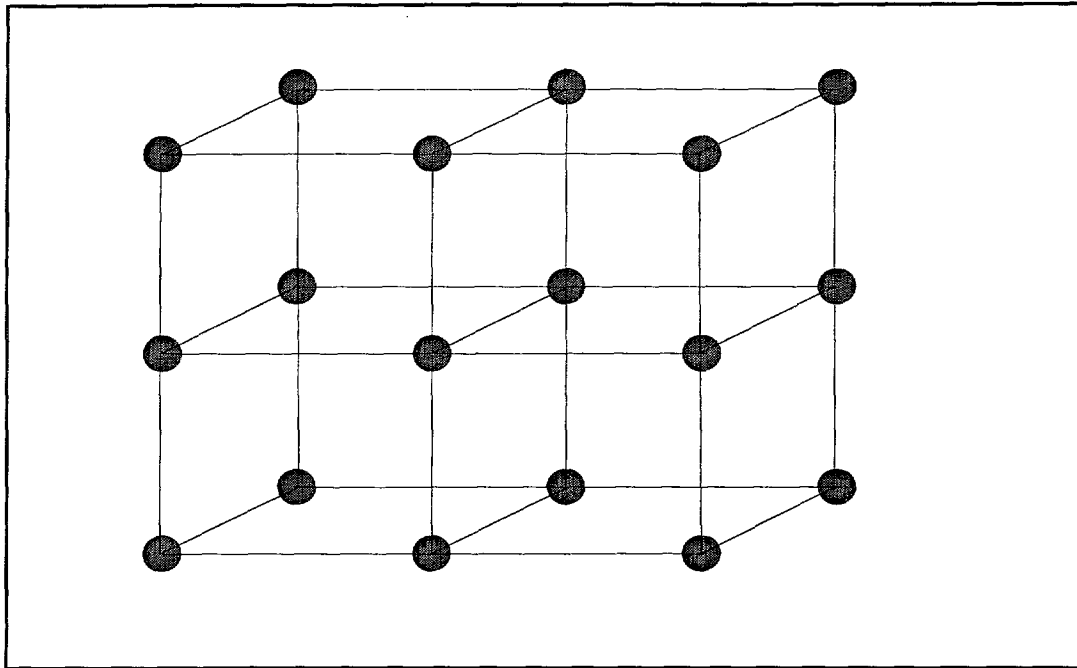


Figure 3: Velocity parameterized on a grid of nodes

One other approach to representing velocity structure worth mentioning is the inversion without blocks of Tarantola and Nercessian (1984). No *a priori* parameterization is assumed, allowing for an essentially arbitrary model solution (Thurber, 1993). The model must eventually be discretized, however, for calculation and visualisation.

1.2 Solving the Forward Problem

In travel time tomography, solution of a forward problem is required in order to determine the ray path and the travel time residual which is to be minimised by inversion. Given a velocity structure and source and receiver locations, the problem usually is to determine the minimum travel time between the two endpoints. This is because first-arrival times are most reliably picked from seismic records since they are not contaminated by signal-generated noise that can complicate the identification and picking of later-arriving phases (Ammon and Vidale, 1993). There are many ways of determining minimum travel times and ray paths. The most appropriate method is often decided by the choice of model parameterization or vice versa (Thurber, 1993). The shooting and bending methods of ray tracing have been popular in the past, but the more recently introduced finite difference methods and network theory techniques are beginning to become popular.

1.2.1 Shooting Method

Ray tracing is a boundary value problem because the two endpoints (source and receiver) are known. The shooting method involves keeping one endpoint fixed and “shooting” the ray out in a specified direction. This initial propagation direction is then modified iteratively until the ray emerges at the target (figure 4). Julian and Gubbins (1977) define a system of six first-order differential equations:

$$\mathbf{r}' = v^2 \boldsymbol{\sigma} \quad (2)$$

$$\boldsymbol{\sigma}' = -\frac{\nabla v}{v} \quad (3)$$

which can be integrated numerically to find the ray path. \mathbf{r} is the position vector and $\boldsymbol{\sigma}$ is the slowness where time (t) is the only independent variable. v is the wave speed. The starting direction which results in the ray passing through the desired endpoint may be determined by solving two nonlinear simultaneous equations:

$$h(i_0, j_0) = H \quad (4)$$

$$g(i_0, j_0) = G \quad (5)$$

h and g are the calculated coordinates of the end of the ray (eg: latitude and longitude) with starting incidence angle i_0 and starting azimuth j_0 . H and G are the coordinates of the end of the correct ray.

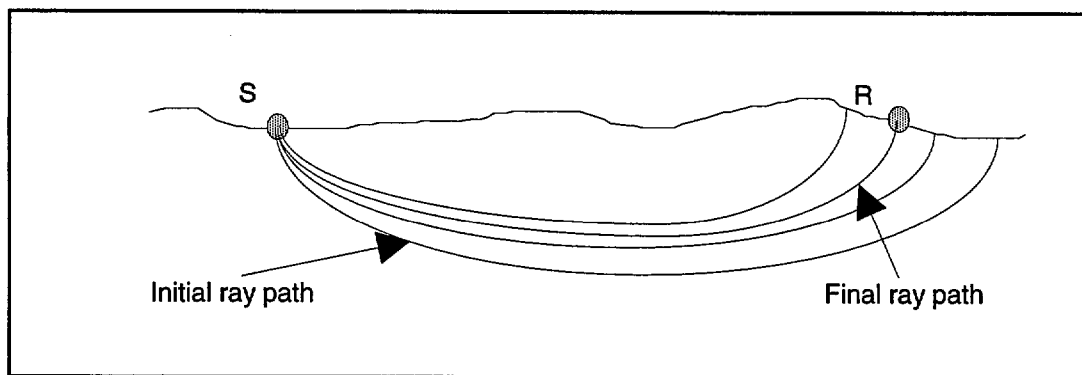


Figure 4: Principle of the shooting method

1.2.2 Bending Method

The bending technique of ray tracing involves keeping both endpoints fixed and perturbing the ray until the true ray path is determined (figure 5). The true ray path occurs when Fermat's principle is satisfied. This principle says that of all the possible

paths joining two points in a medium, the actual ray path is such that the travel time along it is stationary. The ray path can be made stationary by solving a nonlinear system of first order equations with finite difference methods based on the ray equation:

$$\frac{d}{ds} \left(u \frac{d\mathbf{r}}{ds} \right) = \nabla u \quad (6)$$

where $u(\mathbf{r})$ is the slowness, s the arc length and \mathbf{r} the position vector. This approach was adopted by Julian and Gubbins (1977). The ray equation can be derived from the eikonal equation or alternatively, it can be seen to be the Euler-Lagrange equation corresponding to the extremization of the integral which describes travel time in terms of slowness and path length. In their study, Julian and Gubbins (1977) found that bending was computationally much faster than shooting. However, while the bending method works well in cases where there are no discontinuities in wave speed, when discontinuities are introduced, the formation of the problem becomes complex and *a priori* information on the nature of the discontinuities is often required to achieve an acceptable solution. On the other hand, the shooting method, being much less complicated than the bending method, is not overly difficult to apply to complex structures. One reason for this is that the rays used in the shooting method always satisfy Fermat's principle, whereas in the bending method the rays only satisfy Fermat's principle on solution. Sambridge and Kennet (1990) suggest that these factors make bending methods less suited for complex velocity structures than shooting methods.

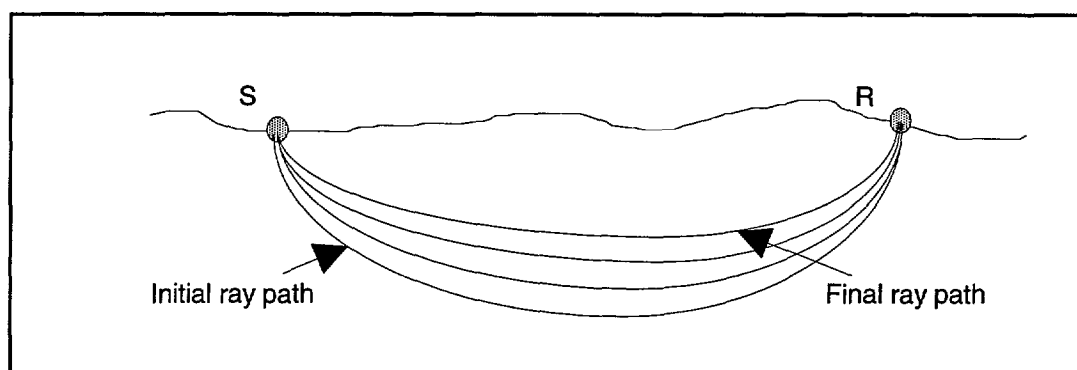


Figure 5: Principle of the bending method

1.2.3 Finite-Difference Method

Finite difference methods represent an alternative approach to the problem of determining ray paths and travel times between source and receiver. They have the advantage of being able to address some of the problems that are inherent in the traditional ray tracing techniques. Both the shooting and bending methods suffer from the possibility of convergence to a local rather than global travel time minimum (Thurber, 1993). Additionally, when a large number of travel paths is required, the computer costs of these two methods become prohibitive. Furthermore, shooting

methods often have trouble finding the correct ray path in a shadow zone. One can appreciate that a method capable of dealing with these problems would be attractive indeed.

Vidale (1988) introduced a scheme based on a finite-difference solution of the eikonal equation that calculated the entire travel time field. Wavefronts are used rather than rays, and the problems associated with ray tracing as outlined above are overcome. The velocity model can be formulated as a grid of points, with equal vertical and horizontal spacing. Figure 6 shows such a grid. Point A is the origin of the seismic waves and consequently is assigned a travel time of zero.

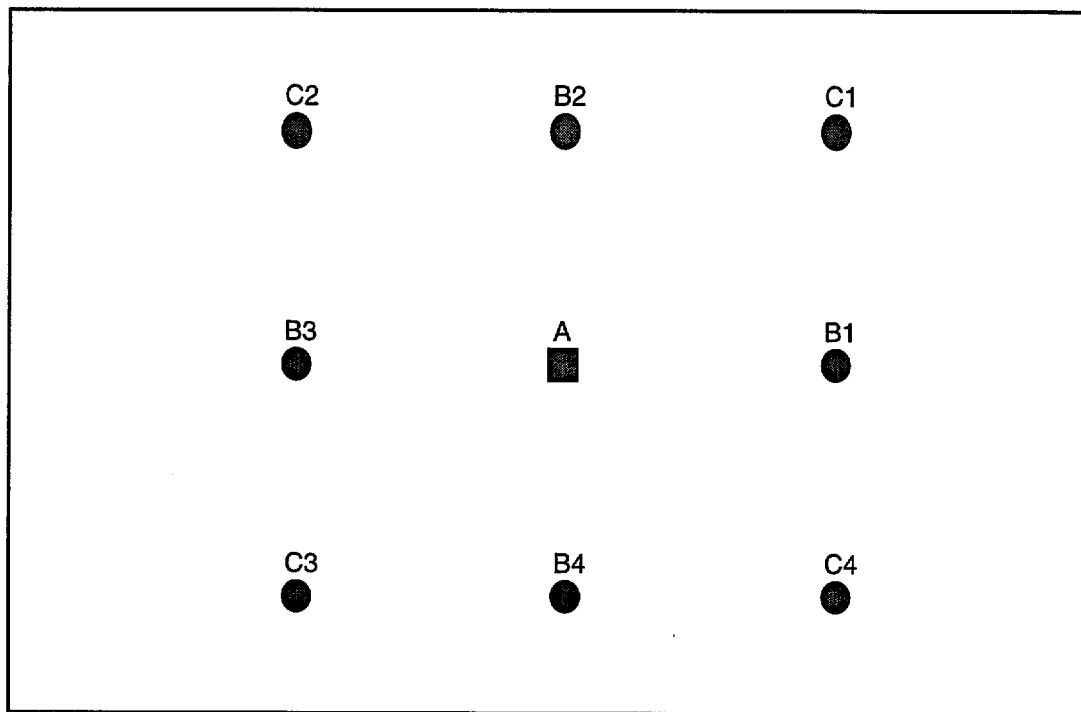


Figure 6: Finite-difference grid

The travel times to the points B1, B2, B3 and B4 are determined by linear interpolation:

$$t_i = \int_A^{B_i} u_A + \left(\frac{u_{B_i} - u_A}{h} \right) ds \quad (7)$$

which has solution:

$$t_i = \frac{h}{2} (u_{B_i} + u_A) \quad (8)$$

h is the grid spacing and u is the known slowness at the nodes indicated by the corresponding subscripts. The travel times to the corner nodes C1, C2, C3 and C4 can be determined by using a finite-difference solution to the eikonal equation. In two dimensions, the eikonal equation can be written:

$$\left(\frac{\partial t}{\partial x}\right)^2 + \left(\frac{\partial t}{\partial z}\right)^2 = u(x, z) \quad (9)$$

This relates the travel time gradient to the slowness at any point in the medium. Using the grid shown in figure 6, it is possible to make central difference approximations of the differential terms shown in equation 9. The procedure is simple and is shown in figure 7. The resulting approximations are:

$$\frac{\partial t}{\partial x} = \frac{1}{2h}(t_0 + t_2 - t_1 - t_3) \quad (10)$$

$$\frac{\partial t}{\partial z} = \frac{1}{2h}(t_0 + t_1 - t_2 - t_3) \quad (11)$$

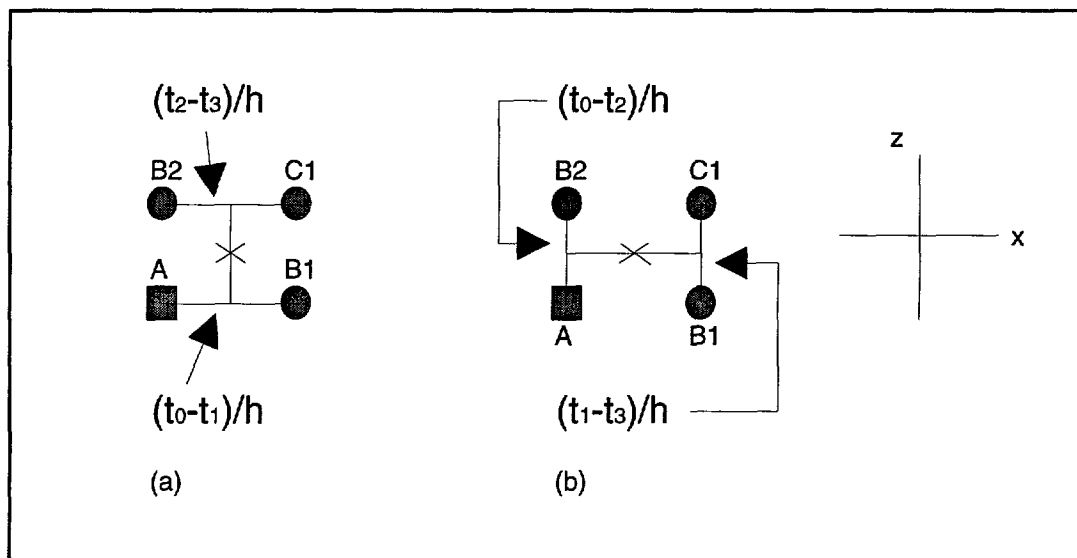


Figure 7: Gradient approximations. (a) $\partial t / \partial x$ is the average of the two differences shown. (b) $\partial t / \partial z$ is the average of the two differences shown. These give equations (10) and (11) respectively.

Substitution of equations (10) and (11) into equation (9) yields the following expression:

$$t_3 = t_0 + \sqrt{2(hs)^2 - (t_2 - t_1)^2} \quad (12)$$

This gives the travel time to point C1 using the travel times from the source to points A, B1 and B2 in a plane wave approximation. Note that point A does not need to be the source point for this equation to be valid. The entire travel time field may be determined using equations (8) and (12). s in equation (12) is the average slowness of all four node points (ie: A, B1, B2 and C1). Once the travel times to the nodes in the first square are calculated, travel times to the remaining nodes are found by expanding the solution region outwards as shown in figure 8. Vidale (1988) also determines a formula applicable to strongly curved wavefronts. In three dimensions, the expanding square method becomes the expanding cube method (Vidale, 1990).

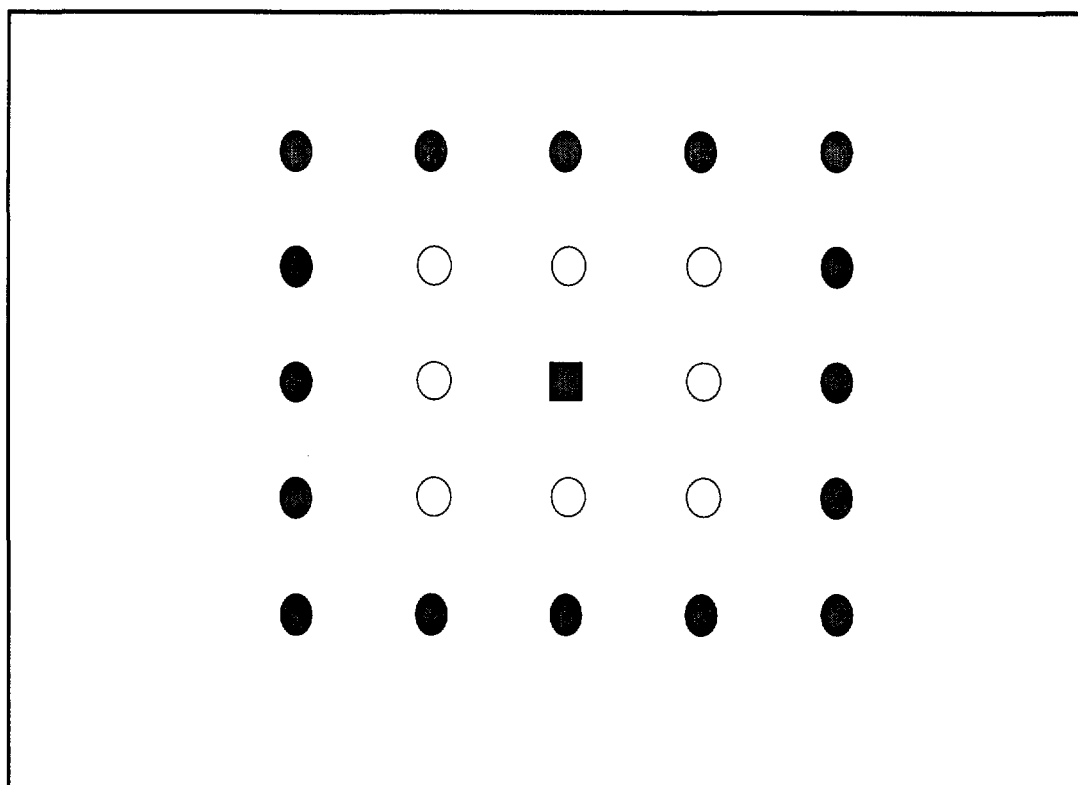


Figure 8: Expanding square method: the travel times to the filled circles are determined from the travel times of the open circles; the filled square is the source point.

The ray paths are found by tracing back through the computed travel time field from the receiver. The travel time field for a single source can be used to trace rays from any number of receivers. If there are a large number of shots and few receivers, then the reciprocity principle of travel times means that receivers can be treated as sources and the travel times to the shot points can be determined. Computation time varies approximately linearly with the number of grid points.

As pointed out by Qin *et al.* (1992), the expanding square method is not very appropriate for models with moderate to large velocity contrasts; causality is violated which can lead

to negative values inside the square root sign. To address this problem, Qin *et al.* (1992) solved the eikonal equation along an expanding wavefront rather than an expanding square. Hole and Zelt (1995) added an extra finite difference operator to Vidale's algorithm that accounted for head waves along the boundary of grid cells. This latter method is quicker and more accurate than that suggested by Qin *et al.* (1992).

1.2.4 Network Method

Network theory can be used to avoid the disadvantages of shooting and bending, and accurately find the global minimum travel time path between source and receiver. By definition, the minimum travel time path through a network will be stationary in time. This means that of all the paths connecting two points in a network, the path of least travel time will satisfy Fermat's principle and hence be (ideally) a true ray path. It is this fact that makes network theory feasible for travel time tomography.

In the network approach of Moser (1991), the subsurface is represented by a large network consisting of points connected by arcs. Each node or point is connected with a restricted number of points in its neighbourhood, but not with points that lie further away. As a result, it is possible to travel from one node to another via the connections. If the nodes of the network are chosen in such a way that almost any ray path can be approximated, then the shortest travel time path between any two nodes should approximate the true ray path between them. A regular grid of nodes will achieve this, and has the added bonus of a considerable saving of memory space. Figure 9(a), taken from Moser (1991), shows a square grid of 25 nodes, each node being connected with at most eight neighbours. Figure 9(b) shows the shortest paths from the upper left node to all other nodes for a homogeneous model. Something to note is that other paths do exist that have equal travel times to the paths shown in figure 9(b). However, in realistic geological situations, if more than one minimum travel time path exists between two points, then it won't be known until the travel time calculations are complete. In his same paper, Moser showed via an example that the network shortest path method was significantly faster than the shooting method in a heterogeneous medium.

A restriction of the network shortest path method is that it can only find the minimum travel time path between two points. In media with complex velocity structures, there may be many ray paths between source and receiver, and even in travel time tomography, it is not always the case that first arrivals are the only waves of interest. Moser (1991) imposes constraints on the shortest path in the event of paths other than the minimum time path being required. If travel times and ray paths of reflected arrivals are needed, then the constraint on the shortest path is that the ray must visit the interface node set. On the occasion that the network used is insufficient for accurately determining the shortest path, the approximation can act as a good initial guess for bending methods.

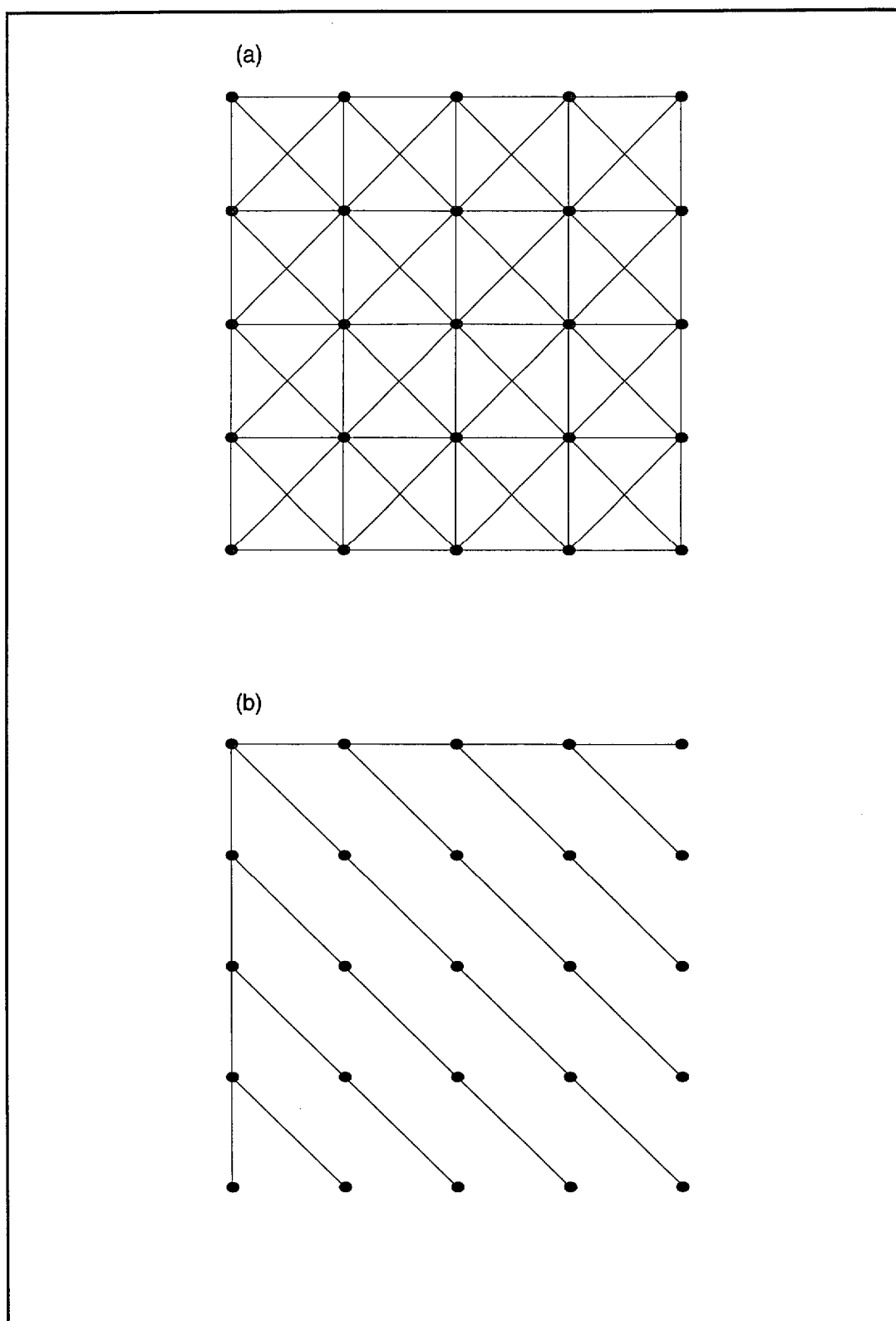


Figure 9: A simple grid demonstrating the principle of network theory. (a) A square grid, with each node connected by at most eight neighbours. (b) Shortest paths from the top left node for a homogeneous medium.(From Moser, 1991)

1.3 Solving the Inverse Problem

Many methods exist for the solution of the inverse problem in seismic tomography. The choice of which is used depends on many factors, including the parameterization employed for the model, the method of solving the forward problem, the nature of the subsurface being modelled, the accuracy of the data and the computer power available. Some commonly used methods include ART (Algebraic Reconstruction Technique), SIRT (Simultaneous Iterative Reconstruction Technique) and Least Squares QR (LSQR), a conjugate gradient technique. Another class of methods, which has been developed more recently, uses random processes to search the model space in order to find better models. These stochastic techniques include the Monte Carlo method, genetic algorithms and Simulated Annealing. All three are global optimization methods, unlike ART, SIRT and LSQR, which are all local optimization techniques. Brief descriptions of all these methods are included in this section.

In travel time tomography, the basis of inversion is the forward problem:

$$t_i = \int_{s_i[u(\mathbf{r})]} u(\mathbf{r}) ds, \quad i = 1, 2, \dots, M \quad (13)$$

where $u(\mathbf{r})$ is the slowness as a function of the position vector \mathbf{r} , t_i is the travel time of the i^{th} ray and s_i is the length of the i^{th} ray path. The inverse problem is to find the slowness field (or velocity field) given the travel times t_i and the source and receiver locations corresponding to the endpoints of all ray paths. The relationship between t_i and u is normally nonlinear, as the integral is performed over the ray path which is dependent on slowness. This relationship can be linearized by considering a small perturbation of the slowness about a reference slowness $u_0(\mathbf{r})$. This produces a travel time given by:

$$t_i = \int_{s_i[u_0(\mathbf{r}) + \delta u(\mathbf{r})]} u_0(\mathbf{r}) ds + \int_{s_i[u_0(\mathbf{r}) + \delta u(\mathbf{r})]} \delta u(\mathbf{r}) ds \quad (14)$$

where $\delta u(\mathbf{r})$ is the linear slowness perturbation. By using Fermat's principle of stationary time, the ray path before and after perturbation will have approximately the same travel time, so $s_i[u_0(\mathbf{r}) + \delta u(\mathbf{r})]$ can be replaced by $s_i[u_0(\mathbf{r})]$, the ray path in the reference slowness field. Replacing the first integral in equation (14) by t_i^0 , the travel time perturbation can be written:

$$\delta t_i = t_i - t_i^0 = \int_{s_i[u_0(\mathbf{r})]} \delta u(\mathbf{r}) ds \quad (15)$$

The ray path $s_i[u_0(\mathbf{r})]$ and travel time t_i^0 can be calculated for the reference slowness model using the methods outlined in section 1.2. The reference slowness model is determined by *a priori* information, and in an iterative inversion procedure, the new reference model is determined from the previous model at each iteration of the inversion. Equation (15) is now a linear relationship between the travel time residual and slowness perturbation and can be used for inversion. An iterative inversion scheme is usually employed to determine the slowness model since equation (15) is a linearization of a non-linear problem.

Following the description by Hole (1992), in a linear problem the data d_i are related to the model $m(\mathbf{r})$ through an integration of the form

$$d_i = \iiint m(\mathbf{r})g_i(\mathbf{r})d\mathbf{r} \quad , \quad i = 1, 2, \dots, M \quad (16)$$

where $g_i(\mathbf{r})$ are the data kernels and the integration covers all of the 3-D space spanned by the model. For a linear inversion to be performed, the model is parameterized as a series of basis functions $h_j(\mathbf{r})$:

$$m(\mathbf{r}) = \sum_{j=1}^N \alpha_j h_j(\mathbf{r}) \quad (17)$$

The data may now be defined by:

$$d_i = \sum_{j=1}^N \alpha_j \Gamma_{ij} \quad (18)$$

where the gamma matrix is given by:

$$\Gamma_{ij} = \iiint h_j(\mathbf{r})g_i(\mathbf{r})d\mathbf{r} \quad (19)$$

The inverse problem now is to solve the linear system of equations (18) to find the unknown parameters α_j . When the model is defined by a set of 2-D or 3-D pixels, the basis functions are unity in the boxes cut by the ray path and zero elsewhere. That is:

$$h_j(\mathbf{r}) = 1 \quad \text{if } \mathbf{r} \text{ is in cell } j \\ = 0 \quad \text{elsewhere}$$

If for example Γ_{ij} is the length of the i^{th} ray in the j^{th} box and d_i is the travel time residual, then α_j will be the slowness perturbation. When there are many rays and many boxes, the inversion of the matrix becomes difficult, and other mathematical techniques are required.

An exact solution to the set of linear simultaneous equations (18) may not be possible. An example is when the problem is overdetermined. In this case, it is possible to employ least squares to find the “best” approximate solution. Here, quotation marks are used for “best” because the least squares criterion implies minimisation of the L_2 norm, which is only one way of quantifying the length of a vector. In its matrix form, equation (18) is:

$$\mathbf{d} = \Gamma \alpha \quad (20)$$

In order to determine the least squares solution, the error E is written as:

$$\begin{aligned} E &= \mathbf{e}^T \mathbf{e} = (\mathbf{d} - \Gamma \alpha)^T (\mathbf{d} - \Gamma \alpha) \\ &= \sum_i^M \left[d_i - \sum_j^N G_{ij} m_j \right] \left[d_i - \sum_k^N G_{ik} m_k \right] \end{aligned} \quad (21)$$

Setting the partial derivatives to zero, ie: $\partial E / \partial m_q = 0$, yields:

$$\Gamma^T \Gamma \alpha - \Gamma^T \mathbf{d} = 0 \quad (22)$$

$\Gamma^T \Gamma$ is a square $N \times N$ matrix and α is a vector of length N so $\Gamma^T \Gamma \alpha$ is a vector of length N . $\Gamma^T \mathbf{d}$ is also a vector of length N . Provided $[\Gamma^T \Gamma]^{-1}$ exists, then the least squares solution to the inverse problem $\mathbf{d} = \Gamma \alpha$ is:

$$\alpha = [\Gamma^T \Gamma]^{-1} \Gamma^T \mathbf{d} \quad (23)$$

To increase the stability of the system, a damping term can be included in equation (23) (Stewart, 1991):

$$\alpha = (\Gamma^T \Gamma + w^2 \mathbf{I})^{-1} \Gamma^T \mathbf{d} \quad (24)$$

where w^2 is the damping parameter. Equation (24) is the damped least squares solution of equation (20). Equations (23) and (24) are normally solved iteratively rather than by trying to invert the respective matrix.

1.3.1 Algebraic Reconstruction Technique (ART)

ART is an iterative procedure which successively changes model parameters for one ray after the other so as to reduce the differences between the observations and the calculations from the model. As formulated by Stewart (1991), the algorithm proceeds by “guessing” an initial model, which normally is based on *a priori* information (eg: refraction survey). From this reference model, the travel time of the first ray is calculated, followed by the corresponding travel time residual (as defined in equation (15)). The reference model is then adjusted by the smallest possible amount, in a least-squares sense, to make it a solution of the first row of the matrix equation. The new solution is then passed on to the second equation where it is again adjusted by the smallest possible amount to make it a solution of the second equation. The process is continued until all the equations have been solved once. It is then a simple matter of returning to the first equation and repeating the procedure again. The iterative procedure is usually halted when the travel time residuals are small enough or when the parameters are not varying significantly. Mathematical derivations of the ART algorithm as applied to travel time tomography can be found in Stewart (1991), Nakanishi (1985), Neumann-Denzau and Behrens (1984) and many other articles.

The algorithm of ART originated in the field of medical science, although it was not called ART then. Early users of ART found it not only slow, but badly conditioned for the typical situation in seismology (Nolet, 1993). Also, ART fails to converge unambiguously in the presence of data errors; a commonplace occurrence with seismic data. A variant of this method, called ARTB, attempts to address some of these problems by basing the iterative back projection version of the linear matrix inversion on the Bayesian optimization criterion (Lees and Crosson, 1992).

1.3.2 Simultaneous Iterative Reconstruction Technique (SIRT)

When solving a system of equations using ART, the solution is updated after each equation is solved. With both SIRT and ART, the difference between observed and calculated travel times (the travel time residual, as defined in equation (15)) is distributed along each ray path as a correction to the slowness in each cell intersected by the ray. In the case of SIRT, unlike ART, this is done *simultaneously* for *all* the rays. If a cell is intersected by more than one ray, then the slowness change attributed to that cell is the average of the slowness perturbations of all the intersecting rays. As in ART, this procedure is repeated after ray tracing through the new field and determining a new set of travel time residuals. The iterative process continues until the travel time residual ceases to decrease significantly between iterations. Mathematical formulations of SIRT may be found in Krajewski *et al.* (1989) and Dueker *et al.* (1993).

SIRT was appropriated from medical imaging technology. Its advantages over ART include speed and stability of convergence. However, it does have several drawbacks, also shared by ART, which include inconsistency and the introduction of nonphysical, *a priori* information into the solution resulting from an implicit rescaling of the problem. Trampert and Leveque (1990) introduce a damped version of the algorithm called DSIRT, which gives complete control of the *a priori* information but at the expense of convergence speed.

1.3.3 Least Squares QR (LSQR) and Conjugate Gradients

The LSQR method is the most efficient method so far available to solve linear tomographic systems, whether overdetermined, underconstrained or both (Nolet, 1993). Although both ART and SIRT converge to some minimum norm solution, they both suffer from the introduction of hidden scaling into the solution, as was mentioned previously. LSQR not only allows the metric to be defined, but in addition has superior convergence speed. A mathematical description of the algorithm can be found in Nolet (1993). Here, the conjugate gradient method based on Scales (1987) will be presented, of which LSQR is a generalisation.

For the conjugate gradient method to be used, the normal equation (equivalent to equation (22)) of equation (20) needs to be considered:

$$\Gamma^T \Gamma \alpha = \Gamma^T d \quad (25)$$

The matrix $\Gamma^T \Gamma$ is square and symmetric and completely characterises the least squares solution of equation (20). If Γ has at least as many rows as columns and is of full column rank (ie: all the column vectors are linearly independent), then the least squares solution of equation (20) is unique. However, if equation (20) is underdetermined or rank deficient, then the least squares solution is not unique. In this case ART and generalised inverse techniques will give the least squares solution whose Euclidean norm is smaller than all other least-squares solutions. The solution to which the conjugate gradient method converges depends upon the initial approximation used. If the initial approximation is zero, then the conjugate gradient algorithm converges to the minimum norm least squares solution.

As will be demonstrated, it is possible to use the conjugate gradient method on equation (25) without explicitly forming $\Gamma^T \Gamma$. This is an important consideration, since $\Gamma^T \Gamma$ will usually be dense even when Γ is sparse. Also, the implicit algorithm converges faster and is more stable than those based on the explicit solution of the normal equations. Another important point is that if the matrix in equation (20) is ill-conditioned, then $\Gamma^T \Gamma$ will be much more ill-conditioned, since its condition number is the square of the condition number of Γ .

If Γ is an $M \times N$ matrix, then the conjugate gradient algorithm may be written as the following: Choose α_0 . Put $s_0 = \mathbf{d} - \Gamma\alpha_0$, $\mathbf{r}_0 = \mathbf{p}_0 = \Gamma^T(\mathbf{d} - \Gamma\alpha_0)$, $\mathbf{q}_0 = \Gamma\mathbf{p}_0$. Then:

$$w_{k+1} = (\mathbf{r}_k, \mathbf{r}_k) / (\mathbf{q}_k, \mathbf{q}_k) \quad (26.1)$$

$$\alpha_{k+1} = \alpha_k + w_{k+1}\mathbf{p}_k \quad (26.2)$$

$$\mathbf{s}_{k+1} = \mathbf{s}_k - w_{k+1}\mathbf{q}_k \quad (26.3)$$

$$\mathbf{r}_{k+1} = \Gamma^T\mathbf{s}_{k+1} \quad (26.4)$$

$$x_{k+1} = (\mathbf{r}_{k+1}, \mathbf{r}_{k+1}) / (\mathbf{r}_k, \mathbf{r}_k) \quad (26.5)$$

$$\mathbf{p}_{k+1} = \mathbf{r}_{k+1} + x_{k+1}\mathbf{p}_k \quad (26.6)$$

$$\mathbf{q}_{k+1} = \Gamma\mathbf{p}_{k+1} \quad (26.7)$$

where $k=0,1,2,\dots$ and the inner product notation $(\mathbf{r}, \mathbf{r}) = \mathbf{r}^T\mathbf{r}$ is used. Note that none of the equations explicitly calculates $\Gamma^T\Gamma$. Instead of subtracting $\Gamma^T\Gamma\alpha$ from $\Gamma^T\mathbf{d}$, the method calculates $\mathbf{d} - \Gamma\alpha$ then multiplies by Γ^T , an equivalent operation according to the laws of matrix algebra. The basic idea behind the conjugate gradient method is minimisation of the quadratic form $f(\mathbf{z}) = (\alpha - \mathbf{z}, \Gamma(\alpha - \mathbf{z}))$. $f(\mathbf{z})$ is positive and is zero if and only if $\mathbf{z} = \alpha$ ie: at the solution. The iterations continue until the residual is small or ceases to change significantly between iterations. The conjugate gradient method is fast, accurate and well designed to take advantage of sparse matrices.

12.

1.3.4 Global Optimization Techniques

One of the characteristics common to all the inversion methods described above is that there is no guarantee of convergence to a global minimum solution. These local methods rely on exploiting the limited information derived from a comparatively small number of models and avoid an extensive exploration of model space. If the subsurface has a complex velocity structure, then local methods depend strongly on the starting model and are prone to entrapment in local minima. As a linearized matrix inverse problem, seismic tomography can exhibit singularity and ill-conditioning.

A different approach to solving the inverse problem is to use random processes to search the model space and find better models. These methods include Monte Carlo, genetic algorithms and simulated annealing, and belong to the class of global optimization techniques. A common attribute of these techniques is that they only require forward modelling (see section 1.2) and calculation of errors. In order to guide the optimization,

it is normal to begin with a number of models representing simple geologic options and then test variations to these models.

If the term Monte Carlo is defined as a purely random search of the parameter space (Sambridge and Drijkoningen, 1992), then when it generates a new model it must neglect the information gained from the sampling of previous models. Model space in seismic tomography is enormous. For example, a typical image may have $20 \times 20 \times 25$ cells, each of which may assume one of 30 different velocity values. The model space in this case has 10,000 dimensions and the number of different models is $30^{10,000}$, larger than the number of atoms in the universe. The Monte Carlo approach will not test every model, but it will spend a significant amount of computation time exploring unfavourable regions of the model space. This usually means that a large number of models must be sampled so Monte Carlo becomes prohibitively slow for large scale problems (Sambridge and Drijkoningen, 1992).

Both simulated annealing and genetic algorithms guide the variations to the initial models by using an analogue to a natural process. Simulated annealing uses an analogy with physical annealing in thermodynamic systems whereas genetic algorithms use an analogy with the genetic evolution of biological systems to optimize the search. Sambridge and Drijkoningen (1992) show that genetic algorithms are inherently superior to Monte Carlo as a method to search model space.

Simulated annealing considers one model at a time and, although many iterations are needed, it can sometimes produce a model faster than genetic algorithms, which consider models in parallel. It works by modelling the cooling of crystals in a melt; in the analogue process, the alignment and movement of atoms depend strongly on the temperature (T). From high T and a great variety of possible states, a crystal gradually cools to a single low energy state. During simulated annealing, a working model is randomly modified between each iteration and each modification is constrained, so is unlikely to eradicate all previous changes. A new model with lower error is always accepted, though a new model with higher error can be accepted conditionally. A more complete description of optimization by simulated annealing can be found in Kirkpatrick *et al.* (1983).

An essential part of the genetic algorithm approach to optimization is that large and complex models are represented by simple binary strings; this means that the model is represented by a pattern of 1's and 0's called bit-strings which can then be manipulated in a manner analogous to the way biological systems evolve at a genetic level to produce more successful organisms. Goldberg (1989) gives an extensive description of genetic algorithms; here an outline based on Drijkoningen and White (1995) is given.

The genetic algorithm approach to the inverse problem, like Monte Carlo and simulated annealing, is nonlinear and optimizes globally. Model parameters are translated into bitstreams (bit-strings) and reproductions, and are modified by cross-overs and mutations. The first step, reproduction, takes a pool of numbers represented by bitstreams and gives each model a fitness value based on its misfit. These fitness values are translated into probability density functions, where good models have a higher probability than poorer models. A random number is then created, and when it falls within the probability interval of the model, the model is allowed through, the process

being continued until the number of final models equals the number of initial models. The second step is called cross-over and involves mixing (cross-over) two parents to create an offspring. Pairs are chosen randomly, as is the cross-over point for each pair, and the ends of the models in each pair are then swapped to create two new models. The final step involves mutation, where occasionally a bit is changed at random. This ensures that some freshness is kept in the pool and prevents premature convergence. The mutation rate is the chance that a bit is changed. The procedure of reproduction, choosing pairs, cross-over and mutation completes one step of the genetic algorithm. A flow chart for this method, taken from Drijkoningen and White (1995), is shown in figure 10. The implicit parallelism which allows information to be communicated between models is a special characteristic of genetic algorithms that make it very powerful.

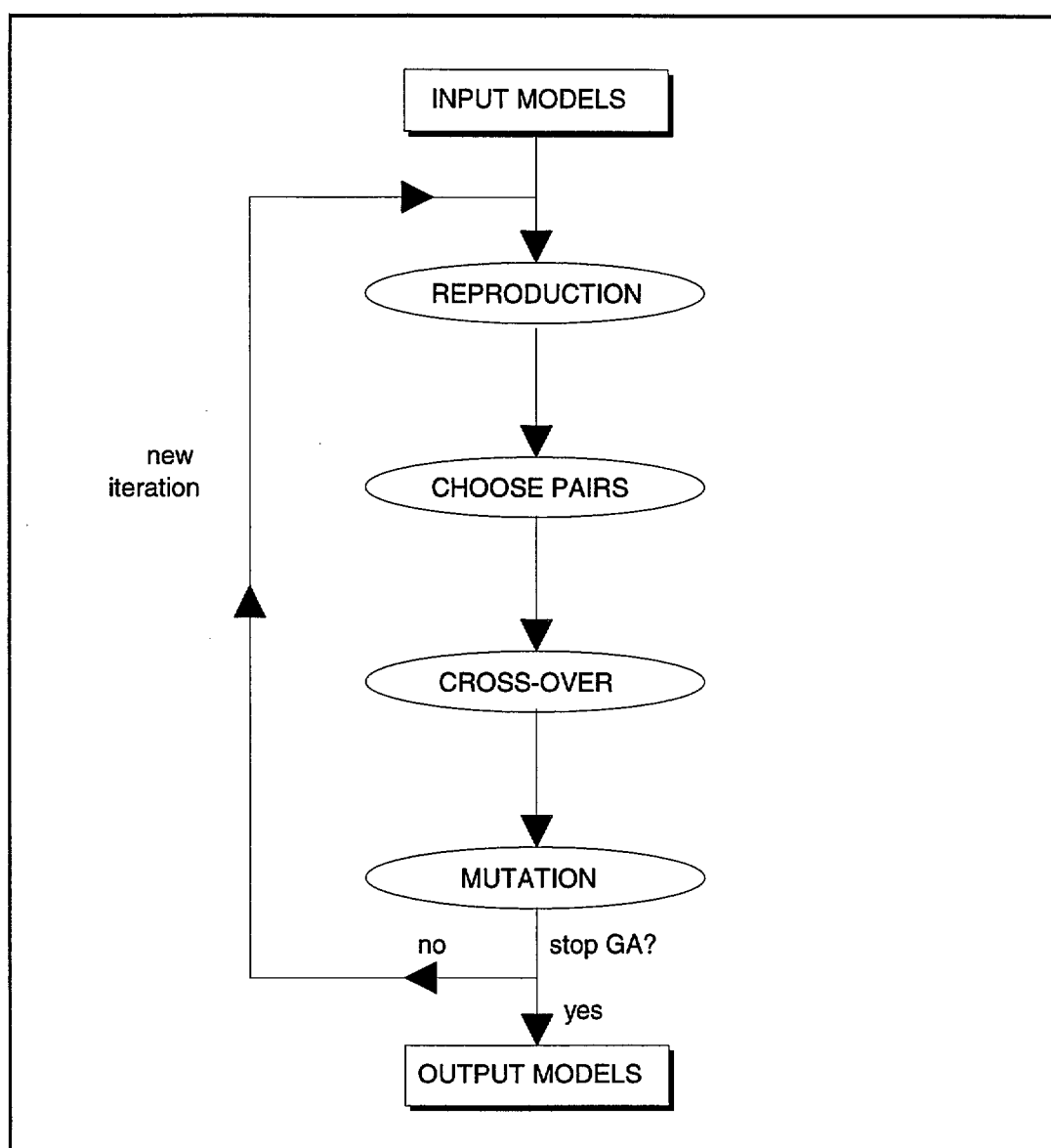


Figure 10: Flow chart of the genetic algorithm (from Drijkoningen and White, 1995)

2 SEISMIC TOMOGRAPHY SOFTWARE

Seismic tomography is a rapidly evolving field of science, and new discoveries and improvements are commonplace. As a result, many of the computer programs associated with it are in a constant state of development, and as such, are only readily used by those with the software development. Tomography codes capable of interpreting three-dimensional seismic data are not common, and those that have a user-friendly interface are rare. This section of the report documents two three-dimensional tomography codes that invert travel times for velocity structure.

“Dogstomo” is a commercial tomography package distributed by Seismic Image Software (SIS). It runs on a PC and has user friendliness as its main attribute. On the other hand, it is quite simplistic and is only capable of limited resolution. The other code is by John Hole (Stanford University) and is distributed for free. It uses more accurate methods than “Dogstomo” and is capable of superior resolution. The main disadvantage of this code is that it is not very user-friendly, with no graphical interface. It also requires programs to be written to input the data. Thus, these two packages contrast each other in user design and the ability to produce high quality results. In essence, the descriptions of the two packages given here reflects their differences, with “Dogstomo” being described mainly in terms of the input steps necessary to produce a tomographic image and on-screen features, while John Hole’s program is described on the basis of the mathematical and geophysical theory it uses and the quality of the inversion it is capable of achieving.

In addition to describing these two packages, a number of other codes that may be of interest are mentioned; these include programs that only solve the forward problem, programs that are yet to be released and programs that have little associated literature.

2.1 “Dogstomo” Software Package

Apart from being capable of doing three-dimensional (3-D) travel time tomography, “Dogstomo” is also able to do two-dimensional (2-D) travel time tomography and two-dimensional amplitude tomography. The software firm that distributes the package, Seismic Image Software (SIS), quoted the price (on 11/12/1995) of “Dogstomo” as US\$2,500 plus a maintenance fee of 18 % per year. While SIS distributes the package, it was actually developed by their sister company in Russia, the Scientific and Production Firm “Development of Geophysical Software” (“DOGS”), hence the name of the package. This creates a problem because the manual is in Russian, with no translation available. However, a file that contains quite detailed information about the program comes with the package and is an acceptable substitute for a manual. There is also an online help system that is quite comprehensive. On the other hand, both of these sources of information tend to be rather cryptic.

For “Dogstomo” to be used, a PC operating under MS-DOS (version 3.0 or higher) with at least a 286 processor is required. Minimum RAM is 1.8Mb and the capacity of the hard disk should be no less than 20Mb; at least 530 kb of free memory must be available for starting the program.

The limited ability of “Dogstomo” to resolve fine structural features is evidenced by the limited number of model parameters allowed. Parameterization is in terms of constant velocity cells, with no more than 10,201 cells permitted. While this number of cells doesn’t sound meagre, it only corresponds to a grid of, for example, 101×101 cells in 2-D or 25×24×17 blocks in 3-D. The number of data that can be processed is unlimited, although no more than 20,402 ray paths can be visualized.

2.1.1 Solving the Tomographic Problem with “Dogstomo”

The approach to solving a tomographic problem using “Dogstomo” is best summarised by the flow chart in figure 11. The coordinates of the sources and receivers and the first arrival travel times between them can be inputted in two different ways. One way is to prepare a file containing all the information, ie coordinates of sources and receivers and first arrival travel times/amplitudes; this file has a conventional extension of #DT. The other option is to place the same material in three different files, with source coordinates, receiver coordinates, and travel times/amplitudes contained in the files with the extensions #SO, #RE and #TT respectively.

For the tomographic problem to be solved, an initial reference model is required (see section 1). By default, the initial model in “Dogstomo” is homogeneous. This may be changed manually by means of a graphical interface to satisfy *a priori* information, or alternatively, the corresponding data may be written into a file. In the case of travel time tomography, the options for an initial model include:

- a 1-D function ie: a set of horizontal layers with the velocity constant in each layer or linearly changing with depth. Discontinuities in velocity are allowed at the interfaces. The extension for the file containing this information is MDL.
- a 2-D function, consisting of a velocity value specified for each cell in a two-dimensional grid. The extension for the file containing this information is VEL.
- a 3-D function, consisting of a velocity value specified for each cell in a three-dimensional grid. The extension for the file containing this information is VEL.

The files containing the source and receiver coordinates, first arrival travel times and initial velocity model embody all of the information necessary to produce a tomographic image. The next step is to solve the forward problem. In the case of travel time tomography, this requires the rays to be traced from source to receiver through the specified velocity model, thus determining minimum travel times and ray paths.

These travel times may be compared with the observed travel times, allowing calculation of the residuals which will be used in the subsequent inversion. The forward modelling

program creates two files. The file with the extension RAY contains the calculated ray paths and travel times. Ray paths may be visualized and the calculated and observed travel times may be plotted for comparison. The file with the extension CEL contains travel time residual data and ray path locations; this information is necessary for inversion.

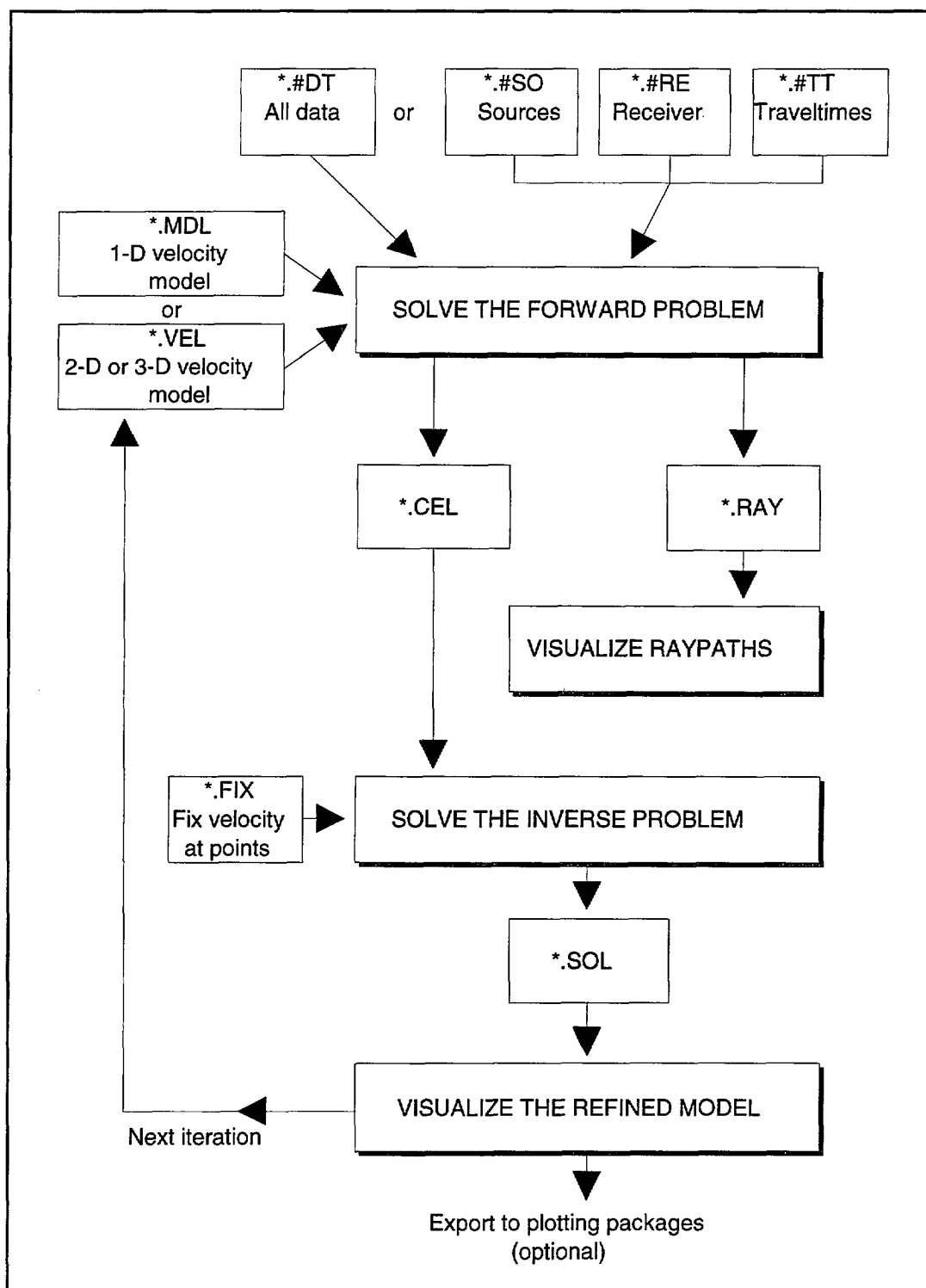


Figure 11: Solving the tomographic problem with "Dogstomo"

Before solving the inverse problem, it may be that the velocities in some regions of the model are known accurately (eg: from acoustic log data). If this is the case, then it is possible to fix these data values so that they will be unchanged by the inversion. This information can be placed in a file with the extension FIX, and acts as a constraint on the inversion process. The inversion step produces a file with the extension SOL, which contains the new values of the velocity parameters. These results may be viewed graphically.

For a two dimensional model, the velocity is displayed on a plane, with different colours corresponding to different velocities. The ray paths may be superimposed onto the velocity model, but they will only be correct if the forward problem is solved again. If the model is three dimensional, then slices in the vertical or horizontal plane may be viewed.

Following the above procedure through once results in a linear tomographic inversion. The non-linear problem can be solved by repeating the cycle, with the velocity model created by the inversion being used as the initial velocity model in the next iteration. The RMS residual can be observed after each cycle to see whether each iteration effects convergence. In addition, a resolution matrix may be displayed.

The graphical display of the refined model is quite simple. It is therefore possible to save the data into graphics files of various formats. The allowed formats are GRD/ASCII/, GRD/binary, GXF, LCT, ZHY and XYZ. These files may then be applied to other plotting packages. In fact, the data at any stage of the tomographic process may be saved in graphics files; this includes ray path, travel time, source/receiver geometry, histogram and resolution matrix information.

Apart from 2-D and 3-D tomographic inversion, 'Dogstomo' also offers 2-D and 3-D kinematic modelling. This is simply the forward part of the tomographic process, and its only difference is that it allows the calculated first arrival travel times to be saved in a text file (extension #DT).

2.1.2 Methods used to Solve the Forward and Inverse Problem

To determine the first arrival travel times and corresponding ray paths from a given velocity structure (ie solving the forward problem), "Dogstomo" uses two different methods depending on the dimensions of the model. In one dimension, the shooting method (see section 1.2.1) is used to determine the transmitted rays. The ray with minimum travel time is kept. If the velocity within a layer changes linearly, then it is discretized into a series of small constant velocity steps.

In two or three dimensions, the velocity model consists of constant velocity cells, but to solve the forward problem, the model is reparameterized as a grid of nodes. The first arrival time from a source node to *all* other nodes is calculated by the theory of graphs (this is the same as network theory), and rays are found by tracing backward from the receivers through the computed travel time field. The velocity between nodes may be

determined either by linear or parabolic (ie: quadratic or second order polynomial) interpolation; the latter being regarded as “high” accuracy and the former as “low” accuracy.

The inverse problem may be solved by one of three methods: backprojection, damped least squares and searching for the smoothest function, the choice being made at the inversion step of the program. These methods will be described in terms of travel time tomography.

Backprojection is the simplest of these methods and works by smearing the travel time residual uniformly along the length of the ray. The slowness perturbation for cell j is the sum of the products of the distance ray i travels in cell j and the slowness perturbation of ray i divided by the sum of the lengths of all rays in cell j . The Algebraic Reconstruction Technique (ART) and Simultaneous Iterative Reconstruction Technique (SIRT) (see sections 1.3.1 and 1.3.2) are in fact iterative formalisms of the backprojection method. If α is defined as the vector of slowness perturbations, with each component divided by the slowness of the corresponding cell of the reference model, that is :

$$\alpha_j = \frac{u_j - u_j^0}{u_j^0}, \quad j=1,2, \dots, N \quad (27)$$

where N is the number of blocks, u_j is the slowness of the new model in the j^{th} block and u_j^0 is the slowness of the reference model in the j^{th} block; and if \mathbf{d} is defined as the vector of travel time residuals, then:

$$\mathbf{d} = \Gamma \alpha \quad (28)$$

This is equation (20) but with the meaning of the matrix and vectors slightly changed. In this case, Γ is the matrix of travel times corresponding to ray i crossing cell j . Equation (28) in component notation is:

$$d_i = \sum_{j=1}^N \Gamma_{ij} \alpha_j \quad (29)$$

which is a special case of equation (18). The backprojection method calculates α_j using the following formula:

$$\alpha_j = \frac{\sum_{i=1}^M \left[\Gamma_{ij} d_i / \sum_{j=1}^N \Gamma_{ij} \right]}{\sum_{i=1}^M \Gamma_{ij}} \quad (30)$$

The advantage of the backprojection technique is that it is very quick and calculates a solution almost instantly. However, the solution quality is very poor and at best reveals only the most anomalous areas inside the investigated region. The velocity values determined by backprojection shouldn't be relied upon.

Damped least squares was described briefly in section 1.3. The expression that is minimized in this case is:

$$p \sum_{j=1}^N \alpha_j^2 + \sum_{i=1}^M \left[d_i - \sum_{j=1}^N \Gamma_{ij} m_j \right]^2 = \min \quad (31)$$

where p is a regularization parameter. The resulting equation is solved using the conjugate gradient method. Damped least squares gives a more reliable result than backprojection but not as quickly. Its main drawback is that the solution values in adjacent cells are independent, which may give rise to unrealistic velocity fluctuations from cell to cell.

The method of searching for the smoothest function attempts to take into account the fact that the velocity values in adjacent cells are likely to be similar. It avoids the salt-and-pepper look that can be obtained by damped least squares. The expression that is minimized in this case is:

$$\frac{p}{2} \sum_{j,k=1}^N \frac{e_{jk} W}{b_{jk}} [\alpha_j - \alpha_k]^2 + \sum_{i=1}^M \left[d_i - \sum_{j=1}^N \Gamma_{ij} \alpha_j \right]^2 = \min \quad (32)$$

where $e_{ij}=1$ if cells j and k have a common side and zero otherwise. W is the area or volume of the cell depending on whether it is 2-D or 3-D respectively and b_{jk} is the distance between the centre of cells j and k respectively. The resulting equation, like the damped least squares approach, is solved by the conjugate gradient method. This is the most time-consuming method, but is the one that usually produces the most geologically realistic result.

The software package "Dogstomo" is recommended for its user-friendly interface and the speed with which it produces results. It can be used to interpret the results of a variety of survey types including cross-borehole, wide-angle refraction and tomographic. However, its limited ability to resolve detailed structure suggests that it would best be used as a means of obtaining a "first look" at the imaged region to aid subsequent modelling using more powerful software.

“Dogstomo” is available from: Seismic Image Software Ltd.
 1100,444 5th Avenue S.W.
 Calgary, Alberta, Canada T2P2T8
 Tel: 403 233 2140
 Fax: 403 266 2685
 Email: sis@tcel.com

2.2 3-D Tomographic Inversion Code by John Hole

This code is designed to determine the velocity structure of a 3-D model by the inversion of travel times. It is designed for Unix machines (eg: Sun and DEC) and uses fairly standard C and Fortran codes suitable for most compilers. The package that is distributed contains 24 files and occupies about 132 Mb of disk space when compiled. Programs need to be written to input data, and since the software provides no graphical means of viewing the results, code needs to be written to convert the output into a format suitable for the 3-D visualization package that will be used.

The tomographic methods on which the code is based are described briefly below. Much of this material is taken from Hole (1992) and to a lesser extent, Hole and Zelt (1995). These publications should be referred to for a detailed description of the methods.

Parameterization of a model is always an important step in solving a tomographic problem. One common problem is that an insufficiently dense parameterization can lead to artefacts in the model. A dense parameterization has inferior resolution of individual model parameters compared to a sparse parameterization, but has superior spatial resolution. The latter quality is preferable because it allows the observation of detailed structure. The code described in this section attempts to invert for densely sampled structure yet minimize the computational cost. The concept of beams for the parameterization is employed, where a ray in two dimensions is redefined as a beam centred on the ray path with amplitude $1/w$ and width w . These beams are used as the data kernels $g_i(\mathbf{r})$ and also as the basis functions $h_j(\mathbf{r})$. In three dimensions the rays are defined as having a cross-sectional area of A and an amplitude of $1/A$. By shrinking the beams to zero width, the slowness perturbation model may be given by:

$$\delta u(\mathbf{r}) = \sum_{j=1}^M \frac{\delta t_j}{l_j} A g_j(\mathbf{r}) \quad (33)$$

where l_j is the total length of the j^{th} ray and δt_j is the travel time residual of the j^{th} ray. The product $A g_j(\mathbf{r})$ is unity along the j^{th} ray and is equal to zero elsewhere. The model $\delta u(\mathbf{r})$ is thus defined only on these infinitesimally thin rays and is unconstrained between them. To obtain a visualization of this model, it is necessary to interpolate the

velocity between the rays. This is also necessary for the forward part of the problem. Equation (33) solves the linear inversion problem of equation (15). To solve the nonlinear problem, iterations are required, with the perturbations determined by equation (33) being added to the reference model. The new model becomes the reference model in the next iteration.

2.2.1 Solving the Forward Problem

The forward problem is solved using a modified form of the finite difference algorithm by Vidale (1990). In his 1990 paper, Vidale extends the 2-D algorithm (explained in section 1.2.3) to 3-D. The principle is the same, the main difference being that the travel time field is calculated by means of an expanding cube rather than an expanding square; this means that several different formulations of equation (12) are required. Hole and Zelt (1995) pointed out some deficiencies in Vidale's algorithm and attempted to correct them. The problems occur when large, sharp velocity contrasts are encountered. In this type of situation, wavefronts are critically refracted at the boundaries between different velocities. Vidale's algorithm does not include finite difference operators that allow head waves to travel along the boundaries between grid cells. In addition, it assumes that waves cannot turn sharply back toward the source. The introduction of head-wave operators will solve the problem of critically refracted waves, and sharply turning waves can be accounted for by setting a flag in the algorithm whenever head-wave operators are used along the faces of the expanding cube. As mentioned earlier, the use of a finite difference scheme such as this calculates the whole travel time field, allowing the minimum travel time and ray path to be calculated between one source and many receivers or vice versa (by the reciprocity principle) using just one set of calculations. This is considerably quicker than ray tracing methods that calculate the travel time of only one source-receiver pair at a time. In addition, the finite difference scheme guarantees that the calculated path will be a global minimum.

The solution to the inverse problem (equation (33)) is based on the model being parameterized as rays. However, the finite difference travel time algorithm requires the model to be parameterized as a grid of nodes. This does not pose any real problems; the linearized travel time inversion described in equation (33) is independent of the method used to find travel times and ray paths, and simply needs to be transformed into the parameterization used in the forward step. In this case, the forward step parameterizes the model at grid points. To achieve a transformation, the value of the model at each grid node is taken to be the average of all the δu_i terms in each of the eight grid cells surrounding the node. One or more rays may pass through a given grid cell so the number of terms to be averaged may be more than eight. This interpolation process also acts to smooth the model.

2.2.2 Solving the Inverse Problem

Equation (33) is a continuous (ie: zero pixel size) version of backprojection that exactly solves the linearized inverse problem. When the model is parameterized at grid points, then:

$$\delta u(\text{node}) = \frac{1}{K} \sum_{k=1}^K \frac{\delta t_k}{l_k} \quad (34)$$

which is equivalent to simple backprojection tomography. When pixels are used as the basis function $h_j(\mathbf{r})$ in equation (17), then the resulting matrix equation (18) may be solved with ART or SIRT which, as was mentioned previously, are in fact just iterative formalisms of backprojection. In the case of nonlinear tomography, where the locations of the rays in the reference model are different to their true locations, a single backprojection is sufficient to approximately solve the linearized inversion problem; the accuracy improving as the grid cell size decreases. Equation (34) can thus be used to solve the linearized inverse problem, and has significant advantages in speed over iterative techniques like ART and SIRT, which require the matrix Γ to be stored.

2.2.3 Examples of Code Applications

John Hole's tomographic inversion code is probably the most commonly used to invert 3-D travel time data from controlled source surveys. Several examples of its use can be found in the literature. Hole (1992) applied his code to the results of a synthetic survey, where the region of interest simulated a low velocity anomaly (such as a zone of partial melt) contained within a 1-D crustal model. 1521 evenly spaced receivers and 9 evenly spaced shots in a 20km×20 km square were used to obtain the data. The velocity model used was 101×101×28 grid points in size, with the separation between nodes being 200m. The algorithm successfully reconstructed the anomaly with good accuracy after 20 iterations. When random Gaussian uncorrelated noise of standard deviation $\sigma = 0.010$ s was added to the data, the anomaly was determined almost as well as when the noise was absent. In both cases, the background velocity model was used as the starting model.

Hole *et al.* (1993a) used the code to interpret 3-D seismic refraction data from western Hecate Strait, British Columbia. Energy from the airgun array sources was recorded at land sites at offsets appropriate to record crustal refraction and wide-angle reflection data; the refraction data were recorded in a broadside geometry. The tomographic inversion algorithm was used to determine the velocity structure of the upper (<12 km) crust. A total of 10,081 first arrival times recorded at seven receivers were used, with the number of recorded shots being well over 1,000. The grid spacing used was 1km in both horizontal and vertical directions. Significant lateral velocity variations were found as a

result of the analysis and their interpretation proved to be consistent with previous studies.

In 1990, a marine seismic experiment designed to study the sedimentary and crustal structure in the Hall Bredning Fjord in East Greenland was carried out by the Alfred-Wegener-Institute. The area of interest was about 100 km by 40 km and the network of marine seismic lines had a total length of roughly 800 km, with an average shot spacing of 50 m. The seismic signals were recorded in a wide angle position by 9 land stations located on the coast surrounding the Fjord. Mandler and Jokat (1995) applied the tomographic inversion code to the first arrival data. The analysis revealed local velocity variations and complex basement contact topography that were not detected by the reflection or in-line refraction analyses. Local velocity highs were interpreted to be caused by the intrusion of magmatic material.

The tomographic inversion code by John Hole is recommended for its minimization of computational costs and ability to converge in the presence of noisy data. Some effort needs to be made to get it operational. In particular, one needs to learn how to input the data and export the results to a suitable visualization package. The accuracy of the algorithm depends partly on the spatial density of the model parameters, with accuracy increasing as node separation decreases. The maximum number of grid points allowed by the code is 4,000,000, but presumably this can be changed depending on the computer power available.

The tomographic inversion code is available from John Hole.
Email: hole@geo.stanford.edu

2.3 Other Related Software

- Inversion Algorithm for a 3-D Refracting Interface: This code is designed to interpret densely sampled broadside refraction data, with first arrival travel times being inverted to determine the structure of a single interface beneath the array. One particularly useful application of this code is to determine the three-dimensional basement structure (this implies depth also) of a sedimentary basin. A description of the algorithm and examples of its applications can be found in Hole *et al.* (1992) and Hole *et al.* (1993b). The code is available from John Hole.
Email: hole@geo.stanford.edu
- 1-D Genetic Algorithm: Although this code is only 1-D, it represents a new approach to the inverse problem by using stochastic methods to find the global minimum solution. The algorithm determines velocity structure using both travel time and waveform information and is described in Drijkoningen and White (1995), in addition to examples of its application. The ocean crust is one situation where the algorithm can be used effectively. The code is available from Guy Drijkoningen.
Email: g.g.drijkoningen@ctg.tudelft.nl

- “NET”: This is a 3-D network ray tracing program that uses the principles outlined in section 1.2.4. True first arrival ray paths and travel times are guaranteed by this algorithm. It can be used to solve the forward part of the travel time tomography problem and is described in Klimes and Kvasnicka (1994). The whole code is written in ANSI-FORTRAN77 but compiling and running the program can take some effort. An associated package called “MODEL” can be used to construct the velocity model. Both codes are available from Michal Kvasnicka.
Email: qasnicka@seis.karlov.mff.cuni.cz
- 3-D Finite Difference Reflection Travel Time Algorithm: This program uses an improved form of the finite difference method of Vidale (1990) to compute reflected travel times. The reflectors can exist at an arbitrary depth between grid nodes. The method is described in Hole and Zelt (1995). The code is available from John Hole.
Email: hole@geo.stanford.edu
- SIGMA 1.0: This software package allows 2-D raytracing, travel-time inversion and amplitude modelling. It is basically a user-friendly version of Colin Zelt’s RAYINVR program and may be used in Windows on a PC or Unix. One feature of this program is that arrival times from significant seismic events may be picked from data stored in SEG-Y files. A graphical model builder is also provided to assist in the creation of a starting velocity model. The price for the package (on 11/12/1995) is US\$5,000. The software is available from Seismic Image Software.
Email: sis@tcel.com
- 3-D Tomographic Inversion Code: This code is by Colin Zelt but is not ready for distribution, so no details have been published at this stage. Apparently, it has many advantages over John Hole’s tomographic inversion code, including speed. For more information, contact Colin Zelt.
Email: czelt@geophysics.rice.edu
- 3-D Tomographic Inversion Code: This code is being developed by Jie Zhang but is not ready for distribution, so no details have been published at this stage. It will be used on data from Mt. Etna, where a 3-D refraction survey has been carried out jointly by MIT and institutes in France and Italy. For more information, contact Jie Zhang.
Email: jie@erl.mit.edu

All the codes mentioned in part 2 of this report have been obtained by AGSO except the ones that have not been released, and only demonstration copies of “Dogstomo” and SIGMA 1.0 have been acquired. The other codes were obtained on the understanding that they were only to be used by AGSO.

ACKNOWLEDGEMENTS

The author wishes to thank Jim Leven for his review of this report, which resulted in many improvements. Thanks also go to Ed Chudyk for his help with software and to the members of the Land Seismic section of AGSO for their general help and encouragement.

REFERENCES

- Aki, K. and Lee, W.H.K. 1976, Determination of three-dimensional velocity anomalies under a seismic array using first P arrival times from local earthquakes, Part 1. A homogeneous initial model. J.Geophys.Res., **81**, p.4381-4399.
- Aki, K. et al. 1977, Determination of the three-dimensional seismic structure of the lithosphere. J.Geophys.Res., **82**, p.277-296.
- Ammon, C.J. and Vidale, J.E. 1993, Tomography Without Rays. Bull.Seism.Soc.Am., **75**, p.509-528.
- Drijkoningen, G.G. and White, R.S. 1995, Seismic velocity structure of oceanic crust by inversion using genetic algorithms. Geophys.J.Int., **123**, p.653-644.
- Duecker, K. et al. 1993, Teleseismic imaging of the western United States upper mantle structure using the simultaneous iterative reconstruction technique. In: H.M. Iyer and K. Hirahara (Editors), Seismic Tomography: Theory and Practice. Chapman and Hall, London, p.265-298.
- Goldberg, D.E. 1989, Genetic algorithms in search, optimization and machine learning, Addison-Wesley, Reading, MA.
- Hawley, B.W. et al. 1981, Simultaneous Inversion for Hypocenters and Lateral Velocity Variations: an Iterative Solution with a Layered Model. J.Geophys.Res., **86**, p.7073-7086.
- Hole, J.A. 1992, Nonlinear High-Resolution Three-Dimensional Seismic Travel Time Tomography. J.Geophys.Res., **97**, p.6553-6562.
- Hole, J.A. 1992, Interface Inversion Using Broadside Seismic Refraction Data and Three-Dimensional Travel Time Calculations. J.Geophys.Res., **97**, p.3417-3429.

Hole, J.A. 1993(a), Interpretation of three-dimensional seismic refraction data from western Hecate Strait, British Columbia: structure of the crust. Can.J.Earth Sci., **30**, p.1440-1452.

Hole, J.A. 1993(b), Interpretation of three-dimensional seismic refraction data from western Hecate Strait, British Columbia: structure of the Queen Charlotte Basin. Can.J.Earth Sci., **30**, p.1427-1439.

Hole, J.A. and Zelt, B.C. 1995, 3-D finite-difference reflection traveltimes. Geophys.J.Int., **121**, p.427-434.

Kirkpatrick, S. et al. 1983, Optimization by Simulated Annealing. Science, **220**, p.671-680.

Krajewski, C. et al. 1989, Iterative Tomographic Methods to Locate Seismic Low-Velocity Anomalies: A Model Study. Geophys.Pros., **37**, p.717-751.

Lee, W.H.K. and Pereyra, V. 1993, Mathematical Introduction to Seismic Tomography. In: H.M. Iyer and K. Hirahara (Editors), Seismic Tomography: Theory and Practice. Chapman and Hall, London, p.9-22.

Lees, J.M. and Crosson, R.S. 1992, Bayesian ART versus conjugate gradient methods in seismic imaging and applications to Mount St Helens, Washington. In: Spatial Statistics and Imaging, Proc. AMS-SIAM Conference.

Mandler, H.A.F. and Jokat, W. 1995, Three-Dimensional Structures of an East Greenland Devonian/Mesozoic Sedimentary Basin as Determined by Tomographic Inversion of Seismic Refraction Data. AGU 1995 Fall Meeting, p.388.

Moser, T.J. 1991, Shortest path calculation of seismic rays. Geophysics, **56**, p.59-67.

Nakanishi, I. 1985, Three-Dimensional Structure Beneath the Hokkaido-Tohoku Region as Derived from a Tomographic Inversion of P-Arrival Times. J.Phys.Earth, **33**, p.241-256.

Neumann-Denzau, G. and Behrens, J. 1984, Inversion of seismic data using tomographic reconstruction techniques for investigation of laterally inhomogeneous media. Geophys.J.R.Astron.Soc., **79**, p.305-316.

Nolet, G. 1993, Solving large linearized tomographic problems. In: H.M. Iyer and K.Hirahara (Editors), Seismic Tomography: Theory and Practice. Chapman and Hall, London, p.227-247.

Qin, F. et al. 1992, Finite-difference solution of the eikonal equation along expanding wavefronts. Geophysics, **57**, p.478-487.

Sambridge, M. and Drijkoningen, G. 1992, Genetic algorithms in seismic waveform inversion. Geophys.J.Int., **109**, p.323-342.

Scales, J.A. 1987, Tomographic inversion via the conjugate gradient method. Geophysics, **52**, p.179-185.

Shalev, E. 1993, Cubic B-Splines: Strategies of Translating a Simple Structure to B-Spline Parameterization. Bull.Seis.Soc.Am., **83**, p.1617-1627.

Stewart, R. 1991, Exploration Seismic Tomography: Fundamentals. Society of Exploration Geophysicists, Tulsa.

Thurber, C.H. 1983, Earthquake Locations and Three-Dimensional Crustal Structure in the Coyote Lake Area, Central California. J.Geophys.Res., **88**, p.8226-8236.

Thurber, C.H. 1993, Local earthquake tomography: velocities and V_p/V_s - theory. In: H.M. Iyer and K. Hirahara (Editors), Seismic Tomography: Theory and Practice. Chapman and Hall, London, p.563-583.

Trampert, J and Leveque, J. 1990, Simultaneous Iterative Reconstruction Technique: Physical Interpretation Based on the Generalized Least Squares Solution. J.Geophys.Res., **95**, p.12553-12559.

Vidale, J. 1988, Finite-Difference Calculation of Travel Times. Bull.Seism.Soc.Am., **78**, p.2062-2076.

Vidale, J. 1990, Finite-difference calculation of traveltimes in three dimensions. Geophysics, **55**, p.521-526.

APPENDIX 1

BIBLIOGRAPHY

The purpose of this bibliography is to provide a guide to some of the literature available on seismic tomography. An effort has been made to emphasize the following aspects of the subject:

- Two and three-dimensional inversion techniques for interpreting seismic tomographic data.
- Application of algorithms pertaining to two and three-dimensional inversion methods to synthetic and real data.
- Inversion algorithms suitable for controlled source tomographic data.

Crosswell tomography and tomography using surface waves, local earthquake P and S waves or normal modes are not considered in general although occasional references are made. Some consideration is given to teleseismic phases as a source in tomography.

A further constraint on this list is that only the most recent publications are used. Exceptions to this occur when the material is considered to be of fundamental importance or when no recent references can be found.

A fair portion of the articles mentioned in the references are contained in this bibliography. The reason for this is that this bibliography exists as a software package. It was constructed using Word Perfect 6.1 and utilizes hypertext. The heading of each paper is highlighted and clicking the mouse on this writing allows the full abstract to be read. Included with the abstract of each paper are some additional comments about the paper and, where possible, the availability of any associated software.

Finally, since there are 96 articles and texts listed, the bibliography has been divided into four sections:

- **3-D Tomography:** This includes methods for the 3-D inversion of data, determination of travel time given a 3-D velocity structure and applications of these methods.
- **2-D Tomography:** This includes methods for the 2-D inversion of data, determination of travel time given a 2-D velocity structure and applications of these methods.
- **Teleseismic Tomography:** The majority of the papers included in this section deal with the application of 3-D inversion techniques to teleseismic data.

- **Miscellaneous:** This contains papers on various aspects of tomography that do not naturally fit into any of the above three categories.

Note that the first two sections correspond to 3-D and 2-D tomography for controlled sources, respectively. This is why the third section, corresponding to teleseismic tomography, stands on its own right. The last section, labelled “miscellaneous”, tends to contain material that is quite theoretical or that deals with specific aspects of application. However, it should be pointed out that much of this material is relevant to the previous sections.

3-D Tomography:

Brac, J. et al. 1989, 3D Tomographic Traveltime Inversion Using 2D or 3D Acquisitions, Surface and Buried Sources. Technical Programme and Abstracts of Papers, European Association of Exploration Geophysicists, **51**, p.107.

Burmakov, Y.A. et al. 1991, Tomographic study of crustal velocity structure in southern Finland. Tectonophysics, **189**, p.29-35.

Durrani, B.A. et al. 1993, An integrated Lithospheric Study of the Colorado Plateau: Part 1 Upper Crustal Velocity Structure Using PACE-1989 Grand Canyon Profile Data and 3-D Tomographic Analysis of the San Francisco Volcanic Field, Northern Arizona. AGU 1993 Fall Meeting, p.412.

Ernest, R. et al. 1985, Least-Squares Inversion of Spatial Seismic Refraction Data. Bull.Seism.Soc.Am., **75**, p.865-880.

Hammer, P.T.C. et al. 1994, Jasper Seamount structure: Seafloor seismic refraction tomography. J.Geophys.Res., **99**, p.6731-6752.

Hole, J.A. et al. 1992, Interface Inversion Using Broadside Seismic Refraction Data and Three-Dimensional Travel Time Calculations. J.Geophys.Res., **97**, p.3417-3429.

Hole, J.A. 1992, Nonlinear High-Resolution Three-Dimensional Seismic Travel Time Tomography. J.Geophys.Res., **97**, p.6553-6562.

Hole, J.A. 1993, Interpretation of three-dimensional seismic refraction data from western Hecate Strait, British Columbia: structure of the Queen Charlotte Basin. Can.J.Earth Sci., **30**, p.1427-1439.

Hole, J.A. et al. 1993, Interpretation of three-dimensional seismic refraction data from western Hecate Strait, British Columbia: structure of the crust. Can.J.Earth Sci., **30**, p.1440-1452.

Hole, J.A. and Zelt, B.C. 1995, 3-D finite difference reflection traveltimes. Geophys.J.Int., **121**, p.427-434.

Hu, G. and Menke, W. 1992, Formal inversion of laterally heterogeneous velocity structure from P-wave polarization data. Geophys.J.Int., **110**, p.63-69.

Ikelle, L.T. 1995, Linearized inversion of 3-D multi-offset data: background reconstruction and AVO inversion. Geophys.J.Int., **123**, p.507-528.

Klimes, L. and Kvasnicka, M. 1994, 3-D network ray tracing. Geophys.J.Int., **116**, p.726-738.

Mandler, H.A.F. and Jokat, W. 1995, Three-Dimensional Structures of an East Greenland Devonian/Mesozoic Sedimentary Basin as Determined by Tomographic Inversion of Seismic Refraction Data. AGU 1995 Fall Meeting, p.388.

Mochizuki, K. et al. 1994, Tomographic Inversion for Seismic Refraction-Reflection Surveys and Its Applications to 1992 Tsushima Basin Experiment. AGU 1994 Fall Meeting, p.424.

Phadke, S. and Kanasevich, E.R. 1990, Seismic tomography to obtain velocity gradients and three-dimensional structure and its application to reflection data on Vancouver Island. Can.J.Earth.Sci., **27**, p.104-116.

Ritter, J.R.R. and Achauer, U. 1994, Crustal tomography of the central Kenya Rift. Tectonophysics, **236**, p.291-304.

Schuster, G.T. and Quintus-Bosz, A. 1993, Wavepath eikonal traveltime inversion: Theory. Geophysics, **58**, p.1314-1323.

Shalev, E. 1993, Cubic B-Splines: Strategies of Translating a Simple Structure to B-Spline Parameterization. Bull.Seism.Soc.Am., **83**, p.1617-1627.

Sneider, R. and Sambridge, M. 1992, Ray perturbation theory for traveltimes and ray paths in 3-D heterogeneous media. Geophys.J.Int., **109**, p.294-322.

Vidale, J. 1990, Finite-difference calculation of traveltimes in three dimensions. Geophysics, **55**, p.521-526.

Wiggins, S.M. et al. 1994, Linearized Limitations of Tomographic Inversion Due to Tomography. AGU 1994 Fall Meeting, p.424.

Zelt, B.C. et al. 1995, Inversion of three-dimensional wide-angle seismic data from the southwestern Canadian Cordillera. To appear in JGR probably early 1996.

Zelt, C.A. 1994, 3-D velocity structure from simultaneous traveltime inversion of in-line seismic data along intersecting profiles. Geophys.J.Int., **118**, p.795-801.

Zhang, J. et al. 1995, Nonlinear Refraction Traveltime Tomography: Imaging Upper Crustal Structure of the Transantarctic Mountains. AGU 1995 Fall Meeting, p.388.

Zhu, H. and Ebel, E. 1991, Tomographic Inversion for the Seismic Velocity Structure Beneath Northern New England Using Seismic Refraction Data. Agu 1991 Fall Meeting, p.297.

Zhu, H. and Ebel, J.E. 1994, Tomographic inversion for the seismic velocity structure beneath northern New England using seismic refraction data. J.Geophys.Res., **99**, p.15331-15357.

Zucca, J.J. 1992, Active High-Resolution Compressional Wave Attenuation Tomography at Newberry Volcano, Central Cascade Range. J.Geophys.Res., **97**, p.11047-11055.

2-D Tomography:

Ammon, C.J. and Vidale, J.E. 1993, J.E. 1993, Tomography Without Rays. Bull.Seism.Soc.Am., **83**, p.509-528.

Bjarnson, I. et al. 1991, Crustal Structure of South Iceland Revealed by Tomographic Inversion of Refraction Data. AGU 1991 Fall Meeting, p.298.

Bjarnason, I. et al. 1993, Tomographic Image of the Mid-Atlantic Plate Boundary in Southwestern Iceland. J.Geophys.Res., **98**, p.6607-6622.

Bloor, R. and Whaler, K. 1994, The generation of near-surface-layer models from seismic reflection traveltimes. Geophys.J.Int., **119**, p.693-705.

Boztepe, E.A. and Braile, L.W. 1994, Kinematic inversion for the 2-D horizontal and vertical qP-wave velocities and depths to interfaces applied to the TACT seismic profile, southern Alaska. Geophys. J.Int., **119**, p.529-547.

Braile, L.W. et al. 1994, Modeling the 2-D seismic velocity structure across the Kenya rift. Tectonophysics, **236**, p.251-269.

Bunks, C. et al. 1995, Multiscale seismic waveform inversion. Geophysics, **60**, p.1457-1473.

Burianyk, M.J. and Kanasevich, E.R. 1995, Crustal velocity structure of the Ominca and Intermontane Belts, southern Canadian Cordillera. J.Geophys.Res., **100**, p.15303-15316.

Caress, D.W. et al. 1992, Tomographic Image of the Axial Low-Velocity Zone at 12°50'N on the East Pacific Rise. J.Geophys.Res., **97**, p.9243-9263.

Dobroka, M. et al. 1992, Tomographic Inversion of Normalized Data: Double-Trace Tomography Algorithms. Geophys.Pros., **40**, p.1-14.

Gohl, K. and Pederson, L.B. 1995, Collisional tectonics of the Baltic Shield in the northern Gulf of Bothnia from seismic data of the BABEL project. Geophys.J.Int., **120**, p.209-226.

Grau, G. and Lailly, P. 1993, Sequential migration-aided reflection tomography: an approach to imaging complex structures. J.Appl.Geophys., **30**, p.75-87.

Greenhalgh, S.A. et al. 1990, Tomographic reconstruction of upper crustal velocity variations in the Arunta Block, central Australia. Tectonophysics, **173**, p.63-72.

Li, L. et al. 1995, Nonlinear Global Optimization of Seismic Refraction Data for 2-D Velocity Structure Using Genetic Algorithms. Agu 1995 Fall Meeting, p.387.

Linping, S. and Haowu, L. 1995, Nonlinear traveltimes Tomography in Anisotropic Media. AGU 1995 Fall Meeting, p.388.

Luo, Y. and Scuster, G.T. 1991, Wave-equation traveltimes inversion. Geophysics, **56**, p.645-653.

Lutter, W.J. et al. 1993, Application of 2-D Travel-Time Inversion of Seismic Refraction Data to the Mid-Continent Rift Beneath Lake Superior. Geophys.Res.Let., **20**(7), p.615-618.

Michelena, R.J. and Harris, J.M. 1991, Tomographic traveltimes inversion using natural pixels. Geophysics, **56**, p.635-644.

Simmons, J.L. and Backus, M.M. 1992, Linearized tomographic inversion of first-arrival times. Geophysics, **57**, p.1482-1492.

Singh, R.P. and Singh, Y.P. 1991, RAYPT- A new inversion technique for geotomographic data. Geophysics, **56**, p.1215-1227.

Turgut, A. A. 1993, TOPOVEL: A FORTRAN Program for Tomographic Inversion of Porosity and Velocity Structure in the Subsurface. Comp. and Geosciences, **19**(4), p.511-532.

Vidale, J. 1988, Finite-Difference Calculation of Travel Times. Bull.Seism.Soc.Am., **78**, p.2062-2076.

Wang, Y. and Houseman, G.A. 1994, Inversion of reflection seismic amplitude data for interface geometry. Geophys.J.Int., **117**, p.92-110.

Wang, Y. and Houseman, G.A. 1995, Tomographic inversion of reflection seismic amplitude data for velocity variation. Geophys.J.Int., **123**, p.355-372.

White, D.J. 1989, Two-dimensional seismic refraction tomography. Geophys.Journ., **97**, p.223-245.

White, D.J. and Clowes, R.M. 1994, Seismic attenuation structure beneath the Juan De Fuca Ridge from tomographic inversion of amplitudes. J.Geophys.Res., **99**, p.3043-3056.

Zelt, B.C. et al. 1993, Crustal velocity structure in the eastern Insular and southernmost Coast belts, Canadian Cordillera. Can.J.Earth Sci., **30**, p.1014-1027.

Zelt, C.A. and Forsyth, D.A. 1994, Modeling wide-angle seismic data for crustal structure: Southeastern Grenville Province. J.Geophys.Res., **99**, p.11687-11704.

Zelt, C.A. and Smith, R.B. 1992, Seismic travelttime inversion for 2-D crustal velocity structure. Geophys.J.Int., **108**, p.16-34.

Teleseismic Tomography:

Achauer, U. 1994, New ideas on the Kenya rift based on the inversion of the combined dataset of the 1985 and 1989/90 seismic tomography experiments. Tectonophysics, **236**, p.305-329.

Aki,K. et al. 1977, Determination of the Three-Dimensional Seismic Structure of the Lithosphere. J.Geophys.Res., **82**, p.277-296.

Benz, H.M. et al. 1992, Lithospheric Structure of Northern California from Teleseismic Images of the Upper Mantle. J.Geophys.Res., **97**, p.4791-4807.

Evans, J.R. and Achauer, U. 1993, Teleseismic velocity tomography using the ACH method: theory and application to continental-scale studies. In: H.M. Iyer and K.Hirahara (Editors), Seismic Tomography: Theory and Practice. Chapman and Hall, London, p.319-360.

Glahn, A. et al. 1993, Southern Rhine Graben: small-wavelength tomographic study and implications for the dynamic evolution of the graben. Geophys.J.Int., **113**, p.399-418.

Spence, W. and Gross, R.S. 1990, A Tomographic Glimpse of the Upper Mantle Source of Magmas of the Jemez Lineament, New Mexico. J.Geophys.Res., **95**, p.10829-10849.

Weiland, C.M. et mal. 1995, Nonlinear teleseismic tomography at Long Valley caldera, using three-dimensional minimum travel time ray tracing. J.Geophys.Res., **100**, p.20379-20390.

Miscellaneous:

Begat, S.L. et al. 1993, Traveltime Tomography in Anisotropic Media. AGU 1993 Fall Meeting, p.419.

Berryman, J.G. 1994, Constraints on minimum velocity variance for seismic-traveltime tomography. *Geophys.J.Int.*, **119**, p.689-692.

Cao, S. and Greenhalgh, S. Calculation of the seismic first-break time field and its ray path distribution using a traveltime tree algorithm. *Geophys.J.Int.*, **114**, p.593-600.

Cao, S. and Greenhalgh, S. 1995, Relative-error-based non-linear inversion: application to seismic traveltime tomography. *Geophys.J.Int.*, **121**, p.684-694.

Carrion, P. 1991, Dual tomography for imaging complex structure. *Geophysics*, **56**, p.1395-1404.

Chiarabba, C. et al. 1995, Upper crustal tomographic images of the Amiata-Vulsini geothermal region, central Italy. *J.Geophys.Res.*, **100**, p.4053-4066.

Delprat-Jannaud, F. and Lailly, P. 1995, Reflection tomography: How to handle multiple arrivals? *J.Geophys.Res.*, **100**, p.703-715.

Doornbos, D.J. 1992, Diffraction and Seismic Tomography. *Geophys.J.Int.*, **108**, p.256-266.

Drijkoningen, G.G. and White, R.S. 1995, Seismic velocity structure of oceanic crust by inversion using genetic algorithms. *Geophys.J.Int.*, **123**, p.653-664.

Hu, G. et al. 1993, A Demonstration of the Joint Use of P wave Polarization and Travel-Time Data in Tomographic Inversion: Crustal Velocity Structure Near the South Iceland Lowland Network. *Geophys.Res.Let.*, **20**(5), p.1407-1410.

Jannaud, L.R. 1995, Travel time inversion with a priori information on illuminated parts of the reflectors. *J.Geophys.Res.*, **100**, p.2151-2160.

Kennet, B.L.N. et al. 1988, Subspace methods for large inverse problems with multiple parameter classes. *Geophys.Journ.*, **94**, p.237-247.

Lindgren, J. et al. 1990, Non-Linear Waveform Inversion of Seismic Data: Retrieving Both Long and Short Wavelength Velocity Information. Technical Programme and Abstracts of Papers, European Association of Exploration Geophysicists, **52**, p.81.

McClain, J.S. and Caress, D.W. 1993, Seismic tomography in marine refraction experiments. In: H.M. Iyer and K. Hirahara (Editors), Seismic Tomography: Theory and Practice. Chapman and Hall, London, p.764-780.

- Mora, P. 1989, Inversion=migration + tomography. *Geophysics*, **54**, p.1575-1586.
- Moser, T.J. 1991, Shortest path calculation of seismic rays. *Geophysics*, **56**, p.59-67.
- Nolet, G. 1993, Solving Large Linearized Tomographic Problems. In: H.M. Iyer and K. Hirahara (Editors), Seismic Tomography: Theory and Practice. Chapman and Hall, London, p.227-247.
- Nowack, R.L. and Braile, L.W. 1993, Refraction and wide-angle reflection tomography: theory and results. In: H.M. Iyer and K. Hirahara (Editors), Seismic Tomography: Theory and Practice. Chapman and Hall, London, p.733-763.
- Phillips, W.S. and Fehler, M.C. 1991, Traveltime tomography: A comparison of popular methods. *Geophysics*, **56**, p.1639-1649.
- Qin, F. et al. 1992, Finite-difference solution of the eikonal equation along expanding wavefronts. *Geophysics*, **57**, p.478-487.
- Qin, F. and Schuster, G.T. 1993, First-arrival traveltime calculation for anisotropic media. *Geophysics*, **58**, p.1349-1358.
- Scarpa, R. 1993, Seismic tomography and modeling of complex geological structures. *J.Appl.Geophys.*, **30**, p.119-130.
- Sambridge, M. and Drijkoningen, G. 1992, Genetic algorithms in seismic waveform inversion. *Geophys.J.Int.*, **109**, p.323-342.
- Schuster, G.T. 1995, Resolution Limits for Refraction Traveltime Tomography. AGU 1995 Fall Meeting, p.388.
- Sneider, R. 1990, A perturbative analysis of non-linear inversion. *Geophys.J.Int.*, **101**, p.545-556.
- Stark, P.B. and Nikolayev, D.I. 1993, Toward Tubular Tomography. *J.Geophys.Res.*, **98**, p.8095-8106.
- Stefani, J.P. 1995, Turning-ray tomography. *Geophysics*, **60**, p.1917-1929.
- Thurber, C.H. 1983, Earthquake Locations and Three-dimensional Crustal Structure in the Coyote Lake Area, Central California. *J.Geophys.Res.*, **88**, p.8226-8236.
- VanDecar, J.C. and Sneider, R. 1994, Obtaining smooth solutions to large, linear, inverse problems. *Geophysics*, **59**, p.818-829.
- Vesnaver, A. 1994, Towards the Uniqueness of Tomographic Inversion Solutions. *J.Seis.Expl.*, **3**, p.323-334.
- Witte, O. et al. 1996, Ray tracing in random media. *Geophys.J.Int.*, **124**, p.159-169.

APPENDIX 2

CONTACTS

This list contains the names, brief details and email addresses of some of the proponents of seismic tomography. Many of the people mentioned have been contacted by the author and have been willing to discuss their research. Where possible, WWW home page addresses are also given. Several research institutions can be found on the internet that make available detailed information on seismic tomography. These home page addresses are listed also.

Guy Drijkoningen: He has done extensive research into the use of genetic algorithms in seismic tomography. Several papers have been published on his findings, two of which are listed in appendix 1 (see Drijkoningen and White, 1995; Sambridge and Drijkoningen, 1992). He has developed a 1D code which is briefly mentioned in this report.

Email: g.g.drijkoningen@ctg.tudelft.nl

Institution: Delft University of technology

Geophysical Tomography Group (GTG): This is a research group within the Department of Seismology at Institut de Physique du Globe de Paris. The GTG is primarily concerned with theoretical and applied geophysics, seismic modelling and inversion of the full waveform and numerical simulation of seismic and volcanic phenomena. They have developed some tomographic codes but they work on massively parallel computers and no effort has been made to create codes that can be used by others.

www: <http://www.ipgp.jussieu.fr/GTG/>

Phil Hammer: As part of his PhD research, he used a spectral tomographic inversion code to model in 3-D the structure of the Jasper Seamount. The data from two seismic refraction experiments were used; these incorporated ocean bottom seismometers and navigated seafloor shots. Bruce Corneulle wrote the original code which was intended for ocean acoustic tomography. It required modifications to allow it to be adapted to seismic refraction tomography. The relevant paper is listed in appendix 1 (see Hammer et al., 1994).

Email: hammer@geop.ubc.ca

Institution: University of British Columbia

John Hole: His principle interest is in the development of practical 3-D seismic inversion algorithms. Some of his codes are documented in section 2 of this report. Currently, he is attempting to determine the deep 3-D structure of the San Andreas Fault system in the San Francisco Bay area and is involved with the acquisition and analysis of 3-D wide-angle seismic data at the Mendocino Triple Junction.

Email: hole@geo.stanford.edu

Institution: Stanford University

www: <http://pangea.stanford.edu/~hole/home.html>

Brian Kennet: He has published several papers on material directly related to seismic tomography. This includes papers on boundary value ray tracing (to solve the forward problem) and subspace methods (to solve the inverse problem).

Email: brian@rses.anu.edu.au

Institution: Australian National University

Kari Komminaho: He is presently working on constructing tomographic images of the Bothnian Bay area as part of BABEL. He uses SEIS83 raytracing program and the inversion program RAYINR (by Colin Zelt) to construct 2-D models. 3-D tomographic inversion is also done, but as yet no details of the program are available.

Email: kko@babel.oulu.fi

Institution: University of Oulu

Michal Kvasnicka: He was involved with the development of the 3-D Network ray tracing program "NET" as described in section 2 of this report.

Email: qasnicka@seis.karlov.mff.cuni.cz

Institution: Charles University

Holger Mandler: As described in section 2.2.3 of this report, Holger Mandler used John Hole's 3-D tomographic inversion program to interpret seismic data collected in the Hall Bredning Fjord in East Greenland. He detected local velocity variations and complex basement contact topography that were not detected by the reflection or in-line refraction analyses.

Email: mandler@geop.ubc.ca

Institution: University of British Columbia

Joe Matarese: An expert in advanced geophysical computing. He did his PhD thesis on nonlinear traveltimes tomography, using finite-difference solutions of the eikonal equation to solve the forward problem and the conjugate gradient method to solve the inverse problem. Current work includes waveform envelope inversion and refraction tomography.

Email: matarese@ncube.com

Institution: nCUBE corporation

www: <http://www-erl.mit.edu/matarese/authorPage.html>

Kimihiro Mochizuki: Has been involved in the field of Ocean Bottom Seismology. He used the results of a 1992 seismic refraction-reflection survey at Tsushima Basin to create tomographic images of the velocity structure beneath the ocean bottom. The pseudo-bending method was used to calculate ray paths for each source receiver pair, and the conjugate gradient method was used to solve the inverse problem.

Email: mochi@eri.u-tokyo.ac.jp

Institution: University of Tokyo

Gerhard Pratt: Works in two areas of seismic tomography. He does research into traveltime inversion in anisotropic media and full waveform inversion. To date, he has only worked on 2-D problems and has specifically concentrated on the cross-borehole problem. He has working software suitable for several applications. In the future he hopes to develop high resolution algorithms for refraction data in 2-D and pursue reflection tomography in 3-D.

Email: g.pratt@ic.ac.uk

Institution: Imperial College of Science, Technology and Medicine

www: <http://diamond.ge.ic.ac.uk/gpratt/www/Welcome.html>

Samizdat Press: This group is devoted to the free distribution of books, lecture notes and software. The current material emphasizes geophysics, with books on geophysical inverse theory, theory of seismic imaging, theoretical seismology etc. that may be downloaded. Jim Berryman has written *Lecture Notes on Nonlinear Inversion and Tomography* which is also available for free.

www: <http://landau.Mines.EDU/~smizdat/>

Malcolm Sambridge: Main research interest is solution of the geophysical inverse problem. He has written a number of papers on non-linear arrival time inversion, subspace methods for large inverse problems and boundary value ray tracing in heterogeneous media. He has also written a paper on applying genetic algorithms to the tomographic problem.

Email: malcolm@rse.su.oz.au

Institution: Australian National University

Gerard Schuster: Current research includes wave equation traveltime and waveform inversion, resolution limits for refraction traveltime tomography and traveltime inversion of both direct and reflected arrivals in VSP data. He heads the Utah Tomography and Modeling/Migration Consortium (UTAM).

Email: schuster@mines.utah.edu

Institution: University of Utah

www: <http://www.mines.utah.edu/~wmschust/>

Albert Tarantola: He is interested in all aspects of theoretical geophysics, particularly inverse problem theory. His theoretical methods for the inversion of geophysical data have been extensively used and published. Presently, he heads the Geophysical Tomography Group.

Email: tarantola@ipgp.jussieu.fr

Institution: University of Paris

Clifford Thurber: The long term focus of his research is the development and application of techniques for three-dimensional seismic imaging using waves from local and distant (teleseismic) earthquakes. His research group has applied seismic tomography to three sections of the San Andreas fault in central California, to Kilauea volcano in Hawaii and to the Ramapo fault zone in New York. He is responsible for several important developments in the field of seismic tomography (eg: the grid approach to parameterization, with the velocity being defined at each node point of the grid and some interpolation function being used to find the velocity at any point between the grid nodes).

Email: clifft@geology.wisc.edu

Institution: University of Wisconsin

www: <http://geology.wisc.edu/thurber.html>

UTAM: This stands for "Utah Tomography and Modelling/Migration Consortium". The aim of this group is to develop innovative tomography and imaging methods for exploration geophysics. A library of modelling, migration and inversion codes is provided to their members; many of the new codes are SEG-Y compatible. Current research includes Wave equation traveltime and waveform inversion, 2-D and 3-D tomostatics and the development of inversion codes. The consortium is headed by Gerard Schuster.

www: <http://www.gg.utah.edu/Facilities/consort/intro1.html>

Barry Zelt: His research focuses mainly on using seismic tomographic inversion techniques to explore the structure of the crust. He has published many papers, including several with John Hole. The 3-D tomographic inversion codes he uses are those developed by John Hole; in 2-D he uses RAYINVR, a code developed by his brother Colin Zelt.

Email: s22baze@gtri.harc.edu

Institution: Geotechnology Research Institute, Houston Advanced Research Center

www: <http://gtri.harc.edu/~s22baze/>

Colin Zelt: Research interests include the development and application of seismic modelling and inversion techniques in the study of the lithosphere and its tectonic evolution. He develops models of the seismic properties of the lithosphere in 2-D and 3-D using artificial source and receiver arrays up to a few hundred kilometres long, both on land and at sea. In most cases, this involves the interpretation of wide-angle seismic refraction/reflection data for the P-wave velocity structure. His 2-D traveltime and amplitude modeling program RAYINVR is widely used. He is currently working on a 3-D tomographic inversion code.

Email: czelt@geophysics.rice.edu

Institution: Rice University

www: <http://zephyr.rice.edu/departments/faculty/zelt/zelt.html>

Jie Zhang: Research interests include Teleseismic SV-wave propagation, Antarctic seismic projects and Refraction traveltime tomography. He has developed two refraction traveltime tomography techniques: one uses Newton's method while the other uses conjugate gradient methods to directly minimize the nonlinear objective function. In both cases, the forward problem is solved using graph-theoretical methods (ie: network methods) to determine first-arrival traveltimes and corresponding raypaths. He is currently developing a 3-D seismic traveltime tomography inversion code for use with refraction data.

Email: jie@erl.mit.edu

Institution: MIT

www: <http://www-erl.mit.edu/~jie/homepage.html>